Theor. Comput. Fluid Dyn. (2006)
DOI 10.1007/s00162-006-0024-z

ORIGINAL ARTICLE

Samuel P. Burns · Adam H. Sobel · Lorenzo M. Polvani

Asymptotic solutions of the axisymmetric moist Hadley circulation in a model with two vertical modes

Received: 19 September 2005 / Accepted: 25 April 2006

Abstract A simplified model of the moist axisymmetric Hadley circulation is examined in the asymptotic limit in which surface drag is strong and the meridional wind is weak compared to the zonal wind. Our model consists of the quasi-equilibrium tropical circulation model (QTCM) equations on an axisymmetric aquaplanet equatorial beta-plane. This model includes two vertical momentum modes, one baroclinic and one barotropic. Prior studies use either continuous stratification, or a shallow water system best viewed as representing the upper troposphere. The analysis here focuses on the interaction of the baroclinic and barotropic modes, and the way in which this interaction allows the constraints on the circulation known from the fully stratified case to be satisfied in an approximate way. The dry equations, with temperature forced by Newtonian relaxation towards a prescribed radiative equilibrium, are solved first. To leading order, the resulting circulation has a zonal wind profile corresponding to uniform angular momentum at a level near the tropopause, and zero zonal surface wind, owing to the cancelation of the barotropic and baroclinic modes there. The weak surface winds are calculated from the first-order corrections. The broad features of these solutions are similar to those obtained in previous studies of the dry Hadley circulation. The moist equations are solved next, with a fixed sea surface temperature at the lower boundary and simple parameterizations of surface fluxes, deep convection, and radiative transfer. The solutions yield the structure of the barotropic and baroclinic winds, as well as the temperature and moisture fields. In addition, we derive expressions for the width and strength of the equatorial precipitating region (ITCZ) and the width of the entire Hadley circulation. The ITCZ width is on the order of a few degrees in the absence of any horizontal diffusion and is relatively insensitive to parameter variations.

Keywords Hadley circulation · Tropical dynamics · Geophysical fluid dynamics

PACS 92.70.Gt, 92.60.Cc, 92.60.Bh, 92.60.Ox, 47.55.Hd, 47.32.Ef

1 Introduction

The Hadley circulation is the axisymmetric component of the meridional (north–south) overturning of the Earth's tropical atmosphere. That is, it is the component of that overturning which results when the flow field

Communicated by R. Klein

S. P. Burns (✉) · A. H. Sobel · L. M. Polvani
Department of Applied Physics and Applied Mathematics, Columbia University, Room 200 S.W. Mudd Building, MC 4701 500 West 120th Street, New York, NY 10027, USA
E-mail: spb25@columbia.edu

Present address: S. P. Burns
The Courant Institute, New York University, Room 1127, 251 Mercer Street, New York, NY 10012, USA
E-mail: sburns@courant.nyu.edu

is averaged in the zonal (east–west) direction. In the annual mean, air rises near the equator, accompanied by copious rainfall as the moisture contained in the warm near-surface air condenses at lower temperatures higher up. This, now dehydrated, upper-level air then flows poleward, and descends at subtropical latitudes, where little rain occurs since the air is dry. The upper-level poleward flow also transports absolute angular momentum, which the equatorial atmosphere generally has in excess at higher-latitude regions due to the rotation of the Earth and the greater distance from the Earth's axis at the equator. This leads to large relative angular momentum, or strong upper-level westerly (eastward) flow relative to the surface, in the subtropical jets at the poleward edges of the circulation. At the edge of the jet the air descends to the surface, where it flows equatorward, losing angular momentum to surface drag. Surface fluxes restore both the angular momentum and humidity of near-surface parcels towards those of the surface, until they ascend again near the equator; the angular-momentum exchange leads to the existence of surface easterlies near the equator and surface westerlies further poleward. These are arguably the most fundamental first-order features of the general circulation of the atmosphere, which dynamical meteorology should be able to explain.

Superimposed on the zonal mean circulation are eddies, or nonaxisymmetric flow features that disappear in the zonal average. These eddies can be quite large, particularly in the extratropics but also in the tropics, and many important features of the general circulation are undeniably related to these eddies. The axisymmetric Hadley circulation is also influenced by eddies, as the flow is nonlinear and eddy transports (rectified wave–wave interaction terms in the zonally averaged equations of motion) can be important to the zonal mean flow. Despite this, axisymmetric models of the Hadley circulation, in which no eddy effects are considered, have been quite useful in building our understanding of the general circulation. Even though there is now increasing evidence that eddies are even more important to the Hadley circulation than previously recognized [25], axisymmetric models will remain a valid starting point. The eddies exist in the first place because the flow which would occur in their absence is baroclinically unstable. Thus studying the axisymmetric circulation is a necessary prerequisite to understanding the complete circulation [18,19].

The vertical structure in studies of the axisymmetric Hadley circulation is of two types. Some studies consider a fully stratified atmosphere, in which the interior of the atmosphere is considered to be nearly inviscid, as described in Schneider [19] and further developed by Held and Hou [7]. This leads to conservation, and homogenization of angular momentum in the interior, and thus to very (in fact unrealistically) strong subtropical jets. Surface drag, however, is essential to the circulation as it restores the angular momentum of near-surface air parcels back to that of the Earth's surface, thus setting the value of the angular momentum for the entire circulation. Because the interior is nearly inviscid, the effects of surface drag are felt only in a thin boundary layer near the surface in these fully stratified models. Other studies consider only a single layer of fluid, obeying a form of the shallow water equations, best thought of as representing only the inviscid upper troposphere [8,9,16,21]. A flow-dependent mass source appears in the equation for the depth of the layer, representing mass transport between the modeled layer and the lower troposphere. In these calculations, surface drag enters implicitly through the value of the angular momentum (or zonal velocity) imputed to the lower-tropospheric mass source that forces the modeled layer.

In contrast to Hadley cell theory, the theory for most other features of the tropical atmospheric circulation favors a spectral, or modal representation of the vertical structure. This is not formally justifiable due to the lack of a discrete upper boundary on the atmosphere (in contrast to the ocean), which prevents the existence of normal-mode solutions, but nonetheless has been shown to give at least qualitatively acceptable results in many circumstances. In many theories, starting from Matsuno [12], only the so-called first baroclinic mode, containing horizontal velocity maxima of opposite sign at the surface and the tropopause with one zero crossing between, is retained. This leads to a set of shallow water equations, but with a different interpretation than that typically used in Hadley cell theory. Rather than representing flow in layers and neglecting vertical structure within each layer, the equations represent the entire tropospheric flow and assume a specific nontrivial form for the vertical structure. Because the first baroclinic mode velocity has a maximum at the surface, it is incapable of representing the interaction of the flow with the surface drag, which acts to bring the near-surface flow to zero without directly affecting upper levels. As shown below, in order to achieve a plausible representation of the interaction with the surface drag, a barotropic or external mode must be added, with a uniform (or at least uniform in sign) velocity throughout the troposphere. In a model with one barotropic and one baroclinic mode, the two modes can cancel at the surface while adding constructively at upper levels, yielding small surface winds and strong upper level winds, in qualitative agreement with observations.

In this study, we analyze the axisymmetric Hadley circulation in a two-mode model of this type, namely the quasi-equilibrium tropical circulation model (QTCM; 13).Our first goal is to make the connection between existing axisymmetric Hadley cell theory, which does not use modal decompositions, and the theory for the

rest of the tropical circulation, much of which does. We have found in numerical simulations with such a model that, for reasonable parameters, the cancelation of the modes at the surface and their constructive addition in the upper troposphere occurs in such a way as to produce a result as close to what is found in fully stratified models as the reduced modal structure allows [2]. These solutions have surface winds that are both small and have the correct latitudinal structure (easterly flow near the equator, westerly further poleward) and upper tropospheric winds characterized by uniform angular momentum at a level near the tropopause. This enhances our confidence in the QTCM and two-mode models generally, but how and why this result occurs is not obvious from inspection of the model equations, and is what we aim to explain in this study.

Our second goal is to understand some key aspects of the role of moisture in the Hadley circulation. Most of the axisymmetric models have considered a dry atmosphere, with moist effects represented implicitly in the choice of an equilibrium temperature profile, postulated to exist in the absence of any circulation. The temperature field is continually relaxed towards the equilibrium profile as the circulation drives the temperature away from it. A few studies with explicit moisture have been done (e.g., [2–5,10,14,15,17]) but the QTCM's reduced vertical structure and simplified (while still complete) physical parameterizations allows the solution to be carried further analytically. One key result from this analysis is that the precipitating region, or intertropical convergence zone (ITCZ) in the QTCM equations has a width and strength that are comparable to those observed in the absence of horizontal diffusion. This is in contrast to a modified version of the model containing a planetary boundary layer, in which the ITCZ width is controlled by diffusion and becomes dramatically stronger and narrower than observed in its absence (Sobel and Neelin, this volume).

The axisymmetric QTCM equations are described in Sect. 2, and in Sect. 3 the inviscid QTCM one-mode and two-mode models are solved to demonstrate that the QTCM equations, with their unique vertical structure functions, are able to recreate the results of previous stratified inviscid models. In Sect. 4 a heuristic derivation of the full dry and moist solutions is mapped out so that the important results of the study are not obscured by the analysis. The dry asymptotic solution is derived in Sect. 5, the moist asymptotic solution is found in Sect. 6. Both models are compared with numerical solutions of the full nonlinear axisymmetric QTCM equations with conclusions in Sect. 7.

2 The quasi-equilibrium tropical circulation model (QTCM)

2.1 The QTCM decomposition

The variables of the QTCM, as described in [13], are obtained by projecting the primitive equations on to a set of vertical structure functions designed to capture much of the observed tropical flow in an economical way. The barotropic momentum variables, $\mathbf{v}_0 = (u_0, v_0)$, and baroclinic momentum variables, $\mathbf{v}_1 = (u_1, v_1)$, are in units of [m/s], and the temperature T and moisture q are expressed in energy units [J/kg] (with c_p absorbed). Because horizontal variations in temperature and moisture are typically small compared to absolute values, these variables are expressed as deviations from constant reference profiles. Assuming axisymmetric, steady solutions, the structures of the QTCM variables are given by:

$$\begin{cases} \mathbf{v}(y,p) = V_0(p)\,\mathbf{v}_0(y) + V_1(p)\,\mathbf{v}_1(y) = V_0(p)\begin{bmatrix} u_0(y) \\ v_0(y) \end{bmatrix} + V_1(p)\begin{bmatrix} u_1(y) \\ v_1(y) \end{bmatrix}, & \text{(a)} \\ T(y,p) = T_{\text{ref}}(p) + a_1(p)\,T_1(y), & \text{(b)} \\ q(y,p) = q_{\text{ref}}(p) + b_1(p)\,q_1(y). & \text{(c)} \end{cases} \tag{1}$$

The model has a rigid lid with the vertical velocity $\omega = 0$ at the upper boundary and the lower boundary is chosen to be an aquaplanet (no land or topography) which gives $\omega = 0$ at the surface. These boundary conditions on ω result in a nondivergent barotropic mode and the vertical velocity is determined only by the baroclinic mode,

$$\omega(y,p) = -\Omega_1(p)\,\nabla\cdot\mathbf{v}_1(y). \tag{2}$$

The vertical structure functions for T are designed to mimic observed tropical profiles, which tend to be close to moist adiabatic throughout the tropics. The vertical profiles for q are less easily justified, but the form of (1c) is nearly equivalent to assuming a fixed vertical profile of relative humidity (note that the actual value of q is not fixed). The barotropic mode of the horizontal velocity is constant with height,

$$V_0(p) = 1. \tag{3}$$

The vertical structure function $V_1(p)$ for the baroclinic mode is derived from $a_1(p)$ by assuming that the pressure gradient term has the same vertical structure as the other linear terms in the baroclinic momentum equation. This leads to

$$V_1(p) = a_1^+(p) - \widehat{a}_1^+, \qquad \text{where } a_1^+(p) = \int_p^{p_s} a_1(\acute{p})\, \mathrm{d}\ln \acute{p}, \tag{4}$$

where p_s is the surface pressure. The constant $\widehat{a}_1^+$, the vertical mean of $a_1^+(p)$, is subtracted so that the vertical integral of $V_1(p)$ is zero. The vertical structure function for ω is found from the baroclinic continuity equation and has the form,

$$\Omega_1(p) = -\int_p^{p_s} V_1(\acute{p})\, \mathrm{d}\acute{p}. \tag{5}$$

It is important to note that there is no surface boundary layer in our model, and surface fluxes are computed using variables evaluated at the surface. In general, values of any quantity at the surface (indicated by the subscript s) and at the top of the atmosphere (indicated by the subscript t) are found by simply evaluating the vertical structure functions at the surface p_s and the nominal tropopause p_t, respectively. Further discussion and justification of the assumed vertical structure functions can be found in Yu and Neelin [26] and Neelin and Zeng [13].

2.2 The axisymmetric moist model

The moist QTCM equations can be reduced to a one-dimensional model by considering axisymmetric steady solutions: this is accomplished by setting $\frac{\partial}{\partial x} = 0$ and $\frac{\partial}{\partial t} = 0$ in the QTCM equations ([13]; eqs. 5.1–5.5). The model here is further simplified by replacing the radiative forcing terms in the temperature equation ([13]; eq. 5.3) with a relaxation towards a given radiative equilibrium profile, $T_\mathrm{R}(y)$, with a relaxation time, τ_R. The turbulent eddy viscosity, ν, and the horizontal diffusion, K_H, are set to zero but the surface drag terms, $1/\tau_\mathrm{D}$, are retained. The QTCM equations with these simplifications become

$$\begin{cases}
\dfrac{\partial}{\partial y}\big(u_1 v_1\big) = -\dfrac{1}{\tau_\mathrm{D}}\, u_s, & \text{(a)}\\[2ex]
\dfrac{\partial v_0}{\partial y} = 0, & \text{(b)}\\[2ex]
v_1 \dfrac{\partial u_0}{\partial y} + \alpha_1\, v_1 \dfrac{\partial u_1}{\partial y} - \alpha_2\, u_1 \dfrac{\partial v_1}{\partial y} - f\, v_1 = -\dfrac{V_{1\mathrm{s}}}{\tau_\mathrm{D}}\, u_s, & \text{(c)}\\[2ex]
\alpha_3 \dfrac{\partial}{\partial y}(v_1^2) + f\, u_1 = -\kappa\, \dfrac{\partial T_1}{\partial y} - \dfrac{V_{1\mathrm{s}}}{\tau_D}\, v_s, & \text{(d)}\\[2ex]
\dfrac{\partial}{\partial y}\left\{M_{Sr1} v_1 + M_{\mathrm{Sp}1} v_1 T_1\right\} = \dfrac{1}{\tau_c^*}\mathscr{H}(q_1 - T_1)\big[q_1 - T_1\big] + \dfrac{1}{\tau_\mathrm{R}}\big(T_\mathrm{R}(y) - T_1\big), & \text{(e)}\\[2ex]
-\dfrac{\partial}{\partial y}\left\{M_{qr1} v_1 + M_{qp1} v_1 q_1\right\}\\[2ex]
\quad = \dfrac{1}{\tau_c^*}\mathscr{H}(q_1 - T_1)\big[T_1 - q_1\big] + \dfrac{1}{\tau_E}\left[1 + \dfrac{\eta^2}{V_\mathrm{s}^2}\,(u_s^2 + v_s^2)\right]^{\frac{1}{2}} \{q_{\mathrm{sat}}(\mathrm{SST}) - q_s\}, & \text{(f)}
\end{cases} \tag{6}$$

where (6a) is the integrated barotropic vorticity equation, (6b) is the barotropic divergence equation, (6c) is the zonal baroclinic momentum equation, (6d) is the meridional baroclinic momentum equation, (6e) is the temperature equation ($\langle a_1 V_1\rangle = M_{Sp1}$ has been used to simplify the left-hand side, and $\langle\rangle$ is the vertical mean in pressure coordinates), (6f) is the moisture equation ($\langle b_1 V_1\rangle = -M_{qp1}$ has been used to simplify the LHS),

$f = 2\Omega \sin\theta$ is the Coriolis parameter, V_{1s} is the surface value of the baroclinic vertical structure function, $p_T = p_s - p_t$ and $\kappa = R/C_p$. The dry static stability M_S as defined in ([13]; eqs. 4.16,4.17,4.18,4.19) has been linearized about T_{ref}, and the gross moist stratification M_q ([13]; eq. 5.10) is linearized about q_{ref}, resulting in

$$\begin{aligned} M_S &= M_{Sr1} + M_{Sp1}\, T_1, \qquad \text{(a)} \\ M_q &= M_{qr1} + M_{qp1}\, q_1. \qquad \text{(b)} \end{aligned} \tag{7}$$

Convection in the QTCM equations is represented by a modified Betts–Miller scheme that reduces convective available potential energy (CAPE) in the column by relaxing the moisture and temperature towards a equilibrium tropical sounding with a timescale τ_C, as described in [13; section 2b]. In the QTCM, the CAPE projected on to the vertical basis functions is expressed as the difference between q_1 and T_1. In this model, convection occurs when the CAPE is positive, $q_1 \geq T_1$, where the $[q_1 - T_1]$ term in (6e) represents convective heating and the $[T_1 - q_1]$ term in (6f) represents convective drying. The onset of convection in the column is controlled by the Heaviside functions, $\mathscr{H}(q_1 - T_1)$, in (6e) and (6f), where

$$\mathscr{H}(q_1 - T_1) = \begin{cases} 1 & \text{if} \quad q_1 \geq T_1 \\ 0 & \text{if} \quad q_1 < T_1 \end{cases} . \tag{8}$$

In equation (6f), the last term on the right-hand side (RHS) is the parameterization of surface evaporation. In the QTCM the evaporation is determined by the difference between the surface moisture and the saturation value at the sea surface. The evaporation also depends on the sum of the surface winds plus a minimum wind speed with a time scale τ_E and the strength of the surface wind dependence controlled by the coefficient η.

In (6a)–(6f), we have defined the time scales

$$1/\tau_D \equiv g\rho_a C_D \frac{V_s}{\langle V_1^2 \rangle p_T}, \qquad 1/\tau_c^* \equiv \frac{1}{\tau_c} \frac{\widehat{a}_1 \widehat{b}_1}{\widehat{a}_1 + \widehat{b}_1}, \qquad 1/\tau_E \equiv g\rho_a C_D \frac{V_s}{p_T}, \tag{9}$$

and the constants

$$\alpha_1 \equiv \langle V_1^3 \rangle / \langle V_1^2 \rangle, \quad \alpha_2 \equiv \langle V_1 \Omega_1 \partial_p V_1 \rangle / \langle V_1^2 \rangle, \quad \alpha_3 \equiv (\alpha_1 - \alpha_2)/2, \quad \alpha_4 \equiv \alpha_1 + \alpha_2, \quad \lambda \equiv -(\alpha_2 + V_{1s}). \tag{10}$$

Finally, in order to discuss angular-momentum conservation, it is useful to construct a combined zonal momentum equation by eliminating $u_1 \partial v_1 / \partial y$ between (6a) and (6c); this has the form

$$v_1 \left\{ \frac{\partial u_0}{\partial y} + \alpha_4 \frac{\partial u_1}{\partial y} - f \right\} = \frac{\lambda}{\tau_D}\, u_s. \tag{11}$$

2.3 The axisymmetric dry model

The dry version of the QTCM equations has no moisture equation (6f), and the effects of moisture are absorbed into an equilibrium temperature function $T_{eq}(y)$. In the temperature equation (6e), the convective heating, $(1/\tau_C^*)\, \mathscr{H}(q_1 - T_1)[q_1 - T_1]$, and radiative cooling, $(1/\tau_R)\, (T_R(y) - T_1)$ are both replaced by a single term that relaxes T_1 towards T_{eq} with a time scale τ_{eq}, yielding

$$\frac{\partial}{\partial y} \left\{ M_{Sr1} v_1 + M_{Sp1} v_1 T_1 \right\} = \frac{1}{\tau_{eq}} \big(T_{eq}(y) - T_1 \big). \tag{12}$$

For the dry model, the momentum equations (6a), (6b), (6c) and (6d) remain unchanged, as they are not explicitly coupled to the moisture q.

2.4 The boundary conditions

In all cases the width of the Hadley cell Y_H is an unknown that is computed as part of the solution. In addition, for the moist case, the width Y_P of the intertropical convergence zone (ITCZ) or convecting region is also an unknown that is computed. Outside the cell, i.e., $y > Y_\mathrm{H}$, the atmosphere is specified to be in radiative equilibrium for the dry model, and radiative–convective equilibrium for the moist model, resulting in the boundary conditions

$$\begin{aligned} T_1(|y| \geq Y_\mathrm{H}) &= T_\mathrm{eq} \qquad \text{(dry case)} \\ T_1(|y| \geq Y_\mathrm{H}) &= T_\mathrm{RCE} \qquad \text{(moist case)} \end{aligned} \tag{13}$$

where T_RCE is the radiative–convective equilibrium temperature in the moist case, and T_eq is the temperature profile towards which T_1 is relaxed relaxes in the dry case (physically, T_eq also represents a radiative–convective equilibrium, but we use a different notation for clarity, since it is applied differently than in the dry case). As a result, the meridional velocity outside the cell satisfies,

$$\begin{aligned} v_0(|y| \geq Y_\mathrm{H}) &= 0, \qquad \text{(a)} \\ v_1(|y| \geq Y_\mathrm{H}) &= 0. \qquad \text{(b)} \end{aligned} \tag{14}$$

For this model, we choose forcing functions such that both T_RCE and T_eq are uniform in y for $|y| > Y_\mathrm{H}$. In the numerical solutions, the model naturally goes to the steady state described by (13) and (14) though no constraint is imposed requiring this to occur; the numerically obtained Y_H need not be the same as that in the analytical solutions, but in practice it is quite close. In the analytical solutions, the temperature and meridional wind are required to go to their equilibrium values continuously at Y_H, but the zonal wind is allowed to be discontinuous, and requires no boundary condition at Y_H. For the equatorially symmetric forcing discussed here, the zonal and meridional winds vanish at the equator and the value of the temperature there is determined from the solution,

$$\begin{aligned} \mathbf{v}_0(y = 0) &= 0, \qquad \text{(a)} \\ \mathbf{v}_1(y = 0) &= 0. \qquad \text{(b)} \end{aligned} \tag{15}$$

For an equatorially asymmetric forcing, neither (15) nor any comparably similar condition holds; the problem becomes somewhat more complex (cf. [20,21,11]) and will not be discussed here. Integrating (6b) and applying the boundary conditions for v_0, (14a) and (15a), results in v_0 vanishing everywhere,

$$v_0(y) = 0. \tag{16}$$

3 Dry inviscid solutions

3.1 The one-mode solution

The baroclinic component of the QTCM, taken in isolation, is isomorphic to the shallow water equations, but its interpretation is different from that usually used in the context of the axisymmetric Hadley circulation. Shallow water systems have been solved in this context [8,9,16], but interpreted as representing the upper-layer flow, rather than as a modal structure giving the entire flow over the troposphere (with opposite signs in the upper and lower tropospheres). The latter interpretation, used in models of the Walker circulation (e.g., [6]), is inappropriate for the Hadley circulation, due to the role of surface drag and the central importance of the barotropic mode. To illustrate this, we start by analyzing the baroclinic component of the QTCM equations in isolation, on an f-plane (f = constant), under a formulation equivalent to that of [16]. In this case, the momentum equations (6c), (6d), and (11), with the barotropic zonal velocity u_0 set to zero, and the dry temperature equation (12) are used. This version of the model is completely inviscid and, as such, $1/\tau_D$ is set to zero. As in PS2002, the weak temperature gradient (WTG) approximation is made [24] and the term $M_{Sp1} v_1 \partial T_1/\partial y$ in equation (12) is neglected. As a consequence the temperature dependent term in the dry static stability (7a) is also be neglected ($M_{Sp1} = 0$), and as a result $M_{Sp1} T_1 \partial v_1/\partial y$ in (12) is neglected too. The dry temperature equation (12) for this one-mode dry model becomes,

$$M_{Sr1}\frac{\partial v_1}{\partial y} = \frac{1}{\tau_{\rm eq}}\left(T_{\rm eq} - T_1\right). \tag{17}$$

The combined zonal momentum equation, (11), with no surface drag and no barotropic mode is

$$v_1\left\{\alpha_4\frac{\partial u_1}{\partial y} - f\right\} = 0. \tag{18}$$

Making the standard assumptions that $v_1 \neq 0$ and $u_1(0) = 0$, equation (18) can integrated for $u_1(y)$,

$$u_1(y) = \frac{f}{\alpha_4}y. \tag{19}$$

The meridional momentum equation (6d), neglecting the first term as is customary in studies of the Hadley circulation, results in geostrophic balance

$$f u_1 = -\kappa\,\frac{\partial T_1}{\partial y}. \tag{20}$$

Equation (20) can be integrated for $T_1(y)$ using the boundary condition (13) with $T_{\rm eq}$ set to zero outside of the cell,

$$T_1(y) = \frac{f^2}{2\kappa\alpha_4}(Y_{\rm H}^2 - y^2), \tag{21}$$

and the meridional velocity is found by integrating (17),

$$v_1(y) = \frac{1}{M_{Sr1}\,\tau_{\rm eq}}\int_0^y \left(T_{\rm eq}(\acute{y}) - T_1(\acute{y})\right)\mathrm{d}\acute{y}. \tag{22}$$

In order to compare with the single-layer solution of [16], the equilibrium temperature distribution $T_{\rm eq}(y)$ is chosen to be a step function,

$$T_{\rm eq}(y) = \begin{cases} \overline{T}_{\rm eq} & \text{for} \quad |y| < Y_{\rm eq}, \\ 0 & \text{for} \quad |y| > Y_{\rm eq}. \end{cases} \tag{23}$$

The width $Y_{\rm H}$ of the Hadley circulation is found by taking the upper limit of the integral in (22) to be $Y_{\rm H}$, and using the boundary condition (14b) to enforce zero net mass across $y = Y_{\rm H}$, implying

$$\int_0^{Y_H} \left(T_{\rm eq}(\acute{y}) - T_1(\acute{y})\right)\mathrm{d}\acute{y} = 0. \tag{24}$$

Using equation (21) for T_1 and (23) for $T_{\rm eq}$, an expression for $Y_{\rm H}$ is found by evaluating the integral in (24),

$$Y_{\rm H} = \left[\frac{3\kappa\alpha_4}{f^2}\,\overline{T}_{\rm eq}Y_{\rm eq}\right]^{\frac{1}{3}}. \tag{25}$$

This expression for the angular momentum conserving $Y_{\rm H}$ is identical to the dimensional form of [16, eq. (10)] up to the dimensionless QTCM constant α_4. Notice, though, that the interpretation is different here. In [16], the solution described only the upper tropospheric flow, whereas here it describes the flow in the entire troposphere. In particular, (19) implies a surface zonal wind roughly as large as the upper tropospheric wind, an unphysical result due to the neglect of surface drag.

3.2 The two-mode solution

The two-mode dry inviscid model is the same as the one-mode model but with the zonal barotropic momentum reintroduced, i.e., $u_0 \neq 0$. As $1/\tau_D$ is still set to zero, it follows that the baroclinic and barotropic modes are uncoupled. This is unphysical, but is done in order to illustrate that the coupling is essential to the solutions we obtain later. The zonal barotropic momentum equation (6a) for the inviscid two-mode model with $1/\tau_D = 0$ is

$$\frac{\partial}{\partial y}\left(u_1 v_1\right) = 0. \tag{26}$$

Equation (26), together with the boundary condition (15) at the equator, has two possible solutions: one with $v_1(y) = 0$ and the other with $u_1(y) = 0$. The first solution is the thermal equilibrium solution as discussed in [7]. For this solution there is no meridional circulation, $T_1 = T_{\rm eq}$ using equation (17), and u_1 is in geostrophic balance with the gradient of $T_{\rm eq}$ using (20). Hide's theorem, as described in [7,18,19], specifies that the maximum in angular momentum must occur at the surface where the generation of angular momentum by friction can balance its export by diffusion. As in the model of [7], the angular momentum everywhere in the domain must be less than or equal to that found at the surface wind at the equator. For a general equilibrium temperature function Hide's theorem will not always be satisfied, and for the $T_{\rm eq}$ used in the one-mode solution, (23), $u_1 = \delta(y - Y_{\rm eq})$, which clearly violates this condition.

The second solution has $u_1(y) = 0$ and the meridional baroclinic momentum equation (6d) is not in geostrophic balance but has the unconventional form,

$$\alpha_3 \frac{\partial}{\partial y}(v_1^2) = -\kappa \frac{\partial T_1}{\partial y}. \tag{27}$$

Equation (27) can be integrated, and applying boundary condition (15b), gives

$$\alpha_3 v_1^2 = -\kappa\, T_1, \quad T_1(0) = 0. \tag{28}$$

The temperature equation (17) for $Y_{\rm E} < y \leq Y_{\rm H}$, using (23) and (28), becomes

$$M_{Sr1} \frac{\partial v_1}{\partial y} - \frac{\alpha_3}{\tau_{\rm eq}\kappa}\, v_1^2 = 0, \tag{29}$$

and has the solution

$$v_1(y) = -\frac{1}{\alpha_3/(\kappa M_{Sr1}\tau_{\rm eq})\, y + c_1}, \tag{30}$$

where c_1 is used to match to the $y \leq Y_{\rm E}$ solution. By inspection, the boundary condition $v_1(Y_{\rm H}) = 0$ implies that $Y_{\rm H} = \infty$, which is unphysical. Note also that we have not solved for u_0, as it is not necessary to do so in order to obtain the baroclinic solution. In the absence of surface drag, the baroclinic and barotropic modes are uncoupled, except in that the consideration of the barotropic mode yields the constraint (26).

3.3 Discussion

Neither of the dry inviscid solutions has a qualitatively acceptable physical structure. Note that (19), given the structure of the baroclinic mode, implies surface zonal winds nearly as large as the upper tropospheric zonal winds in the single-mode solution. This is inconsistent with observations, and is an artifact of the neglect of surface drag. Adding finite surface drag to this single-mode model, however, would damp the upper tropospheric winds as much as the surface winds, also inconsistent with observations. Adding a barotropic mode in the absence of surface drag also yields problematic solutions, which either violate Hide's theorem or have no baroclinic zonal wind, strongly violating geostrophic balance and giving an infinite extent to the circulation. The correct physical behavior requires the two modes to be coupled by surface drag. This allows the solution to develop both weak surface winds, strong nearly angular momentum-conserving zonal winds aloft and a finite cell width. For the following dry and moist models, two velocity modes are retained and the nonzero surface drag term, $1/\tau_{\rm D} \neq 0$, is included in the momentum equations (6a), (6c), (6d) and (11).

4 Heuristic derivation of solutions with surface drag

The procedure for obtaining asymptotic solutions to (6) is described in detail in the next section; here, for the sake of clarity a heuristic derivation is given so the essential results are not obscured by the analysis. In the previous section it was shown that the purely inviscid two-mode solution corresponds to an unphysical circulation. In this section, in order to obtain a physically meaningful solution, the surface drag terms are retained on the right-hand side of (6a), (6c), (6d) and (11); the turbulent eddy viscosity and the horizontal diffusion (ν and K_{H} respectively in [13]) are still neglected. Beginning with the combined zonal momentum equation, (11), it is assumed that, to leading order, both sides of the equation are equal to zero. This yields the desired result that surface winds are weak (but nonzero after we go to next order) while a form of angular-momentum conservation holds in the upper troposphere, as is found in fully stratified, axisymmetric, nearly inviscid solutions (e.g., [7]). On the RHS of (11) the zonal surface winds are assumed to equal zero at leading order. This results in the barotropic zonal wind's being proportional to the baroclinic zonal wind and allows τ_{D} to be finite,

$$u_s = u_0 + V_{1s}u_1 = 0. \tag{31}$$

To leading order the left-hand side (LHS) of equation (11) is also assumed to vanish,

$$v_1 \left\{ \frac{\partial u_0}{\partial y} + \alpha_4 \frac{\partial u_1}{\partial y} - f \right\} = 0. \tag{32}$$

Equation (32) is inviscid only inasmuch as interior friction is neglected. It is justified, somewhat counterintuitively, by assuming that $1/\tau_{\mathrm{D}}$ is *large*; this renders u_s so small that the RHS of (11) can be neglected at leading order, in spite of the fact that u_s is multiplied by the same large drag coefficient. (32) states that, if v_1 is nonzero, the absolute vorticity must vanish at a level where the basis function, $V_1(p)$, is equal to α_5. Equivalently, it can also be viewed as a statement of angular-momentum conservation at that level. For standard QTCM parameters, the level in question is approximately 300 hPa, 100 hPa below the nominal tropopause. Approximate angular-momentum conservation at this level was found in the QTCM numerical solutions of Burns and Sobel [2]. In fully stratified solutions, axisymmetric circulations conserve, and thus homogenize, angular momentum throughout the free troposphere within the circulation; equivalently, they have zero absolute vorticity there and (32) is the QTCM equivalent of this. The assumed modal structures do not allow zero absolute vorticity, uniform angular momentum, or any other such constraint to hold throughout the troposphere for any solution which has a baroclinic component; a relation such as (32) is the closest analog which is possible to the fully stratified angular momentum constraint. Expressing u_0 in terms of u_1 from the zero surface wind condition (31), the LHS of (11) becomes

$$v_1 \left\{ (\alpha_4 - V_{1s}) \frac{\partial u_1}{\partial y} - f \right\} = 0. \tag{33}$$

Assuming v_1 is nonzero in the interior of the Hadley cell, the leading order solution for u_1 is found from equation (33) by integrating the terms in the bracket. The leading order balance in the meridional baroclinic momentum equation (6d) is assumed to be geostrophic,

$$f u_1 = -\kappa \frac{\partial T_1}{\partial y}, \tag{34}$$

and (34) can be integrated for T_1.

In the analysis developed above, the dry and moist models are the same, because we have not considered the temperature equation, but, beyond this point, we must consider the dry and moist models separately. For the dry model, the temperature equation (12) is used. Once T_1 is known, (12) can be integrated for v_1, and solutions can be found for both the nonlinear and linearized forms of (12). The similarity between the linear and nonlinear solutions justifies the use of the WTG approximation [24]. The width of Hadley cell Y_{H} is found, as in the one-mode solution, by evaluating the integral for v_1 at Y_{H} and using the boundary condition $v_1(Y_{\mathrm{H}}) = 0$. Finally, once u_1 and v_1 are known, the correction to the zonal surface winds can then be found from the next-order barotropic zonal momentum equation,

$$\frac{\partial}{\partial y}(u_1 v_1) = -\frac{1}{\tau_{\mathrm{D}}} u_s^{(1)}, \tag{35}$$

The moist model retains the moisture equation (6f) and uses the temperature equation (6e). The nonlinear terms on the LHS of (6e) and (6f) scale as the temperature gradient and will be neglected. The meridional surface wind dependence of the surface evaporation will be shown to be small, and using the leading order zero zonal surface wind result (31), the WTG version of the moisture equation (6f) reduces to

$$-M_{qr1}\frac{\partial v_1}{\partial y} = \frac{1}{\tau_c^*}\mathscr{H}(q_1 - T_1)\big[T_1 - q_1\big] + \frac{1}{\tau_E}\left\{q_{\rm sat}({\rm SST}) - q_s\right\}, \tag{36}$$

and the WTG version of the temperature equation (6e) is

$$M_{Sr1}\frac{\partial v_1}{\partial y} = \frac{1}{\tau_c^*}\mathscr{H}(q_1 - T_1)[q_1 - T_1] + \frac{1}{\tau_{\rm R}}\big(T_{\rm R}(y) - T_1\big). \tag{37}$$

Equations (36) and (37) are both piecewise linear, and can be solved for q_1 and v_1 in the convecting ($q_1 \geq T_1$) and nonconvecting ($q_1 < T_1$) regions of the cell. The cell width is again found by imposing $v_1(y = Y_{\rm H}) = 0$, and the width of the convecting region, $Y_{\rm P}$, is determined by locating the point where the $T_1(y) = q_1(y)$. The asymptotic results derived for both the dry and moist models will be shown to be in close agreement with a numerical model of the full nonlinear system (6a)–(6f).

5 Dry solution with surface drag

The asymptotic analysis sketched above, is here carried out in detail for the dry model with no turbulent eddy viscosity ($\nu = 0$) and no horizontal diffusion ($K_{\rm H} = 0$) but with the surface drag $1/\tau_{\rm D}$ retained. The scales used are described first, followed by the nondimensional equations with a parameter ε, which is small for small values of $\tau_{\rm D}$ and meridional winds that are weak compared to the zonal winds, as is observed for the zonal mean tropical circulation. The leading order solution is determined, as well as the next order correction to the zonal surface winds and an analytic expression for $Y_{\rm H}$, the width of the circulation. Numerical solutions of the full nonlinear system are presented and the asymptotic solutions are shown to be in close agreement with the numerical results. The dry temperature equation (12) is used with an equilibrium temperature of the form,

$$T_{\rm eq}(y) \equiv \Lambda\,{\rm sech}^2(\sigma y) + \overline{T}_{\rm eq}. \tag{38}$$

The form the equilibrium temperature used here is designed to represent a forcing confined to the tropics, as opposed to the global cosine-squared forcing used in [7].

5.1 Scale analysis

The following scales are used to nondimensionalize the variables of the dry system, where tildes are used to indicate dimensional scales and starred variables are nondimensional:

$$u_0 = \widetilde{U}u_0^*, \quad u_1 = \widetilde{U}u_1^*, \quad v_1 = \widetilde{V}v_1^*, \quad y = \widetilde{L}y^*, \quad T_1 = \widetilde{T}\,T_1^*. \tag{39}$$

A beta plane is used to approximate the Coriolis parameter f as a Taylor series about the equator, i.e., $f = \beta\widetilde{L}\,y^*$, where $\beta = 2\,\Omega/r_{\rm e}$, and $r_{\rm e}$ is the radius of the Earth.

The length scale $\widetilde{L}$ is chosen to be the equatorial deformation radius,

$$\widetilde{L} = \sqrt{\frac{c}{2\beta}} = \left[\frac{1}{2\beta}\sqrt{\frac{\kappa M_{Sr1}}{\widehat{a}_1}}\right]^{1/2}, \tag{40}$$

where c is the gravity-wave speed for the QTCM equations [22], and is given by

$$c = \sqrt{\frac{\kappa M_{Sr1}}{\widehat{a}_1}}. \tag{41}$$

Angular-momentum conservation ($\partial u_1/\partial y \sim \beta\, y$) is used to relate the zonal wind scale, $\widetilde{U}$, to $\widetilde{L}$,

$$\widetilde{U} = \beta\, \widetilde{L}^2 = \frac{1}{2}\sqrt{\frac{\kappa M_{Sr1}}{\widehat{a}_1}}. \tag{42}$$

Assuming that geostrophy forms the dominant balance in the meridional baroclinic momentum equation (6d), the scale for the temperature variations, $\widetilde{T}$, is

$$\widetilde{T} = \frac{\widetilde{U}\beta\widetilde{L}^2}{\kappa} = \frac{\beta^2\widetilde{L}^4}{\kappa}. \tag{43}$$

A WTG balance is assumed in the temperature equation (12), $M_{Sr1}\partial v_1/\partial y \sim 1/\tau_{\rm eq}(T_{\rm eq}(y) - T_1)$. The WTG balance also implies that the dry static stability, M_S, is constant to leading order, resulting in the following scale for the meridional wind,

$$\widetilde{V} = \frac{\widetilde{T}\,\widetilde{L}}{\tau_{\rm eq} M_{Sr1}}. \tag{44}$$

Although under a strict WTG assumption the scale for $T_{\rm eq}$ should be larger than that for T_1 [24], for the Hadley circulation a strict interpretation of WTG is not appropriate and the temperature variation over the circulation is comparable to, if smaller than by an order-unity factor, the equilibrium temperature variation [16]. Thus, $\tilde{T}$ is used as the scale for $T_{\rm eq}$, i.e., $T_{\rm eq} = \widetilde{T}\, T^*_{\rm eq}$, and the RHS of (12) also scales as $\widetilde{T}$, so that

$$\frac{1}{\tau_{\rm eq}}\big[T_{\rm eq}(y) - T_1\big] \sim \frac{\widetilde{T}}{\tau_{\rm eq}}. \tag{45}$$

5.2 Nondimensionalization

The scales defined in Sect. 5.1 are substituted into equations (6a), (6c), (6d) and (12), which become

$$\begin{cases} \varepsilon\,\dfrac{\partial}{\partial y}\big(u_1^* v_1^*\big) = -u_s^*, & \text{(a)} \\ \varepsilon\left[v_1^*\dfrac{\partial u_0^*}{\partial y^*} + \alpha_1\, v_1^*\dfrac{\partial u_1^*}{\partial y^*} - \alpha_2\, u_1^*\dfrac{\partial v_1^*}{\partial y^*} - \dfrac{1}{\rm Ro}\, v_1^* y^*\right] = -V_{1s}\, u_s^*, & \text{(b)} \\ \alpha_3\,\varepsilon\,\delta\,\dfrac{\partial (v_1^{*^2})}{\partial y^*} + \dfrac{1}{\rm Ek}\, y^* u_1^* = -\dfrac{1}{\rm Ek}\,\dfrac{\partial T_1^*}{\partial y^*} - \delta\, V_{1s}\, v_1^*, & \text{(c)} \\ \dfrac{\partial}{\partial y}\left\{v_1^* + \varpi\, v_1^* T_1^*\right\} = T^*_{\rm eq} - T_1^*. & \text{(d)} \end{cases} \tag{46}$$

Several dimensionless parameters appear in the above equations; these parameters are now discussed. The equatorial Rossby number Ro, defined by

$$\mathrm{Ro} \equiv \frac{\widetilde{U}}{\beta\widetilde{L}^2}, \tag{47}$$

is equal to one given our choice of scaling for $\widetilde{U}$, and thus will not be referred to beyond this point. The small parameter ε, defined by

$$\varepsilon \equiv \frac{\widetilde{V}^2/\widetilde{L}}{\widetilde{V}/\tau_{\rm D}} = \frac{\tau_{\rm D}\,\widetilde{V}}{\widetilde{L}} \ll 1, \tag{48}$$

is the ratio of the meridional advective terms to the surface-drag terms in the momentum equations and typically is of order 10^{-2}. Using the scales defined in the previous section for $\widetilde{U}$ and $\widetilde{L}$, and for typical values of $1/\tau_{\rm D}$ the ratio of the zonal advective terms to the surface drag terms in the zonal momentum equations (6a) and (6c) is of order one,

$$\frac{\widetilde{U}^2/\widetilde{L}}{\widetilde{U}/\tau_{\rm D}} = \frac{\tau_{\rm D}\,\widetilde{U}}{\widetilde{L}} \sim 1. \tag{49}$$

The momentum aspect ratio, δ, is defined as the ratio of the meridional velocity scale to the zonal velocity scale, and can be shown to be of order ε by expressing it as the ratio of (48) over (49) yielding

$$\delta \equiv \frac{\widetilde{V}}{\widetilde{U}} = \frac{\tau_{\rm D}\,\widetilde{V}/\widetilde{L}}{\tau_{\rm D}\,\widetilde{U}/\widetilde{L}} \sim \varepsilon. \tag{50}$$

The zonal Ekman number, Ek, defined to be the ratio of the surface drag force to the Coriolis term, can be shown to be order one using (47) and (49),

$$\mathrm{Ek} \equiv \frac{\widetilde{U}}{\widetilde{U}\tau_{\rm D}\,\beta\widetilde{L}} = \frac{\widetilde{U}}{\beta\widetilde{L}^2}\,\frac{\widetilde{L}}{\tau_{\rm D}\,\widetilde{U}} = \frac{\widetilde{L}}{\tau_{\rm D}\,\widetilde{U}} \sim 1. \tag{51}$$

ϖ is defined to be a nondimensional parameter called the weak temperature gradient (WTG) number, and is the ratio of the horizontal temperature advection term to the vertical advection term,

$$\varpi \equiv \frac{M_{Sp1}\widetilde{T}\,\widetilde{V}/\widetilde{L}}{M_{Sr1}\widetilde{V}/\widetilde{L}} = \frac{M_{Sp1}}{M_{Sr1}}\,\widetilde{T} \ll 1. \tag{52}$$

After nondimensionalizing, the combined zonal momentum equation (11) becomes

$$\varepsilon v_1^* \left\{ \frac{\partial u_0^*}{\partial y^*} + \alpha_4 \frac{\partial u_1^*}{\partial y^*} - y^* \right\} = \lambda\, u_s^*. \tag{53}$$

Note that the RHS of (53) and (46a) differ by a factor of λ, which is determined by the model's vertical structure functions, and from [13] has a value of approximately 0.2, which is of order $\epsilon^{1/2}$. Since λ is dependent on the model structure, it is not truly an adjustable parameter, as are, for example, the Coriolis parameter, convective time scale, etc. Thus it is not strictly appropriate as a small parameter for asymptotic analysis (it cannot be sent to zero), but using it as such is essential to derive a consistent solution that lies in the desired physical regime as determined from fully stratified solutions. Physically, we wish to neglect surface drag in the combined barotropic–baroclinic momentum equation (53), in order to obtain an angular momentum conservation law, while retaining it in the barotropic momentum equation (46a), so that we can have both u_1 and v_1 nonzero. By assuming $\lambda \sim \epsilon^{1/2}$, we can make this happen. To leading order the zonal winds near the tropopause will be angular momentum conserving, the surface winds will vanish, and the first nonzero correction to the zonal surface winds will then be obtained from equation (46a). In the following we let $\lambda = \lambda'\varepsilon^{1/2}$ with $\lambda' \sim 1$. After substituting for λ', (53) becomes

$$\varepsilon^{1/2} v_1^* \left\{ \frac{\partial u_0^*}{\partial y^*} + \alpha_4 \frac{\partial u_1^*}{\partial y^*} - y^* \right\} = \lambda'\, u_s^*. \tag{54}$$

Thus, at $O(1)$, u_s^* will vanish as discussed below.

5.3 Asymptotic solutions

In order to find a perturbation solution to the dry Hadley circulation the dependent variables are expanded in one half powers of the small parameter ε. As shown in (50), δ scales as ε so the variables may be expanded in powers of ε only,

$$\begin{cases} u_0^* = \varepsilon^0 u_0^{(0)} + \varepsilon^{1/2} u_0^{(1/2)} + \varepsilon^1 u_0^{(1)} + \cdots & \text{(a)} \\ u_1^* = \varepsilon^0 u_1^{(0)} + \varepsilon^{1/2} u_1^{(1/2)} + \varepsilon^1 u_1^{(1)} + \cdots & \text{(b)} \\ v_1^* = \varepsilon^0 v_1^{(0)} + \varepsilon^{1/2} v_1^{(1/2)} + \varepsilon^1 v_1^{(1)} + \cdots & \text{(c)} \\ T_1^* = \varepsilon^0 T_1^{(0)} + \varepsilon^{1/2} T_1^{(1/2)} + \varepsilon^1 T_1^{(1)} + \cdots & \text{(d)} \end{cases} \tag{55}$$

Recall that $v_0 = 0$ (see equation (16)) and thus need not be expanded or carried further. Also, the dry system (46) is solved for both $\varpi \sim O(1)$ and $\varpi \sim O(\varepsilon)$ to examine the validity of the WTG assumption. Substituting (55) into (46) and collecting similar powers of ε yields the characteristic asymptotic sequence of problems which we now discuss.

At order $O(\varepsilon^0)$, (46a) and (46b) both give the result that the leading order barotropic and baroclinic components of the surface zonal wind cancel at the surface, i.e.,

$$u_0^{(0)} + V_{1s} u_1^{(0)} = 0. \tag{56}$$

The meridional baroclinic momentum equation (46c), at order $O(\varepsilon^0)$, is an equation for geostrophic balance between the zonal baroclinic wind and the temperature gradient,

$$y^* u_1^{(0)} = -\frac{\partial T_1^{(0)}}{\partial y^*}, \tag{57}$$

and the dry temperature equation (46d), at $O(\varepsilon^0)$, is

$$\frac{\partial}{\partial y^*}\left\{ v_1^{(0)} + \varpi\, v_1^{(0)} T_1^{(0)} \right\} = T_{\mathrm{eq}}^* - T_1^{(0)}. \tag{58}$$

At this order $u_0^{(0)}$ and $u_1^{(0)}$ are still undetermined due to the degeneracy in equations (46a) and (46b). To solve the leading order system, the order $O(\varepsilon^{1/2})$ momentum equations must be considered.

At order $O(\varepsilon^{1/2})$, the zonal barotropic momentum equation (46a) gives that the order $O(\varepsilon^{1/2})$ zonal surface winds are also equal to zero,

$$u_s^{(1/2)} = 0, \tag{59}$$

and the combined zonal momentum equation (54), using (59), becomes

$$v_1^{(0)} \left\{ \frac{\partial u_0^{(0)}}{\partial y^*} + \alpha_4 \frac{\partial u_1^{(0)}}{\partial y^*} - y^* \right\} = \lambda'\, u_s^{(1/2)} = 0. \tag{60}$$

The leading order dry solutions can now be obtained from equations (56), (57), (58) and (60), and take the simple form

$$\begin{cases} u_1^{(0)}(y^*) = \dfrac{\mu}{2}\, y^{*2}, & \text{(a)} \\ u_0^{(0)}(y^*) = |V_{1s}| \dfrac{\mu}{2}\, y^{*2}, & \text{(b)} \\ T_1^{(0)}(y^*) = -\dfrac{\mu}{8}\, y^{*4} + T_1^{(0)}(0), & \text{(c)} \\ v_1^{(0)}(y^*) = \dfrac{1}{1 + \varpi\, T_1^{(0)}} \displaystyle\int_0^{y^*} \left(T_{\mathrm{eq}}^* + \frac{\mu}{8}\, \acute{y}^4 - T_1^{(0)}(0) \right) \mathrm{d}\acute{y}, & \text{(d)} \\ u_s^{(0)} = 0, \quad u_s^{(1/2)} = 0, & \text{(e)} \end{cases} \tag{61}$$

where $\mu \equiv 1/(\alpha_4 - V_{1s})$. The constant $T_1^{(0)}(0)$ is determined by the boundary condition (13), and is found to be

$$T_1^{(0)}(0) = \frac{\mu}{8}\, Y_{\mathrm{H}}^4 + \overline{T}_{\mathrm{eq}}^*. \tag{62}$$

The equilibrium temperature profile $T_{\mathrm{eq}}(y^*)$, given by (38), is chosen to have maximum amplitude Λ, a value of $\overline{T}_{\mathrm{eq}}$ away from the equator and a width σ. Using (38) and (61c), the leading order meridional wind $v_1^{(0)}(y^*)$ is computed from (61d), and is given by

$$v_1^{(0)}(y^*) = \frac{1}{1 + \varpi\, T_1^{(0)}} \left[\frac{\Lambda^*}{\sigma} \tanh(\sigma y^*) + \frac{\mu}{40}\, y^{*5} - \frac{\mu}{8}\, Y_{\mathrm{H}}^4\, y^* \right]. \tag{63}$$

Finally, the value of Y_{H} is obtained by enforcing the boundary condition (14b) using (63), which gives

$$\frac{\Lambda^*}{\sigma}\tanh(\sigma Y_{\mathrm{H}}) - \frac{\mu}{10}Y_{\mathrm{H}}^5 = 0. \tag{64}$$

This is transcendental in Y_{H} but, assuming $\sigma Y_{\mathrm{H}} \gg 1$, $\tanh(\sigma Y_{\mathrm{H}})$ can be approximated by 1 so that

$$Y_{\mathrm{H}} \approx \left\{\frac{10\Lambda^*}{\sigma\mu}\right\}^{1/5}. \tag{65}$$

This result has the same form as in [19, eq. 20] for a continuously stratified atmosphere, and as in [16] for a β-plane model. This correspondence gives us confidence that the expansion used here is reasonable. The width of the Hadley circulation found here for a hyperbolic secant-squared forcing is less sensitive to Λ than in [7], where Y_{H} is proportional to the square root of the amplitude of the forcing. This difference may be due to the fact that the forcing in [7] is global, where as T_{eq} here is limited to tropics.

Having solved the order $O(\varepsilon^0)$ system, the first nonzero correction to the zonal surface winds $u_s^{(1)}(y^*)$ are found from the order $O(\varepsilon^1)$ zonal barotropic momentum equation (46a)

$$u_s^{(1)} = -\frac{\partial}{\partial y}\left(u_1^{(0)}v_1^{(0)}\right), \tag{66}$$

using (61a) for $u_1^{(0)}$ and (63) for $v_1^{(0)}$. This calculation of the surface zonal winds is similar to that described by Lindzen and Hou [11].

5.4 Comparison with numerical solution

A numerical code has been written to solve the time-dependent full nonlinear axisymmetric dry equations: (6a), (6c), (6d) and (12). The model uses explicit differencing for the spatial derivatives with an upwind scheme for terms involving meridional advection at a resolution of 8.9 km. A staggered leapfrog scheme is used for the time derivatives with a Robert filter and a time step of 30 s. The numerical solution has horizontal diffusion in the momentum equations but with $K_{\mathrm{H}} = 500\,\mathrm{m}^2/\mathrm{s} \sim \varepsilon^2\widetilde{L}^2$. The meridional boundary conditions are walls at 40° on each side of the equator, which does not affect the steady solution since it vanishes outside of the cell at about 20°. The model is initialized with zero winds and $T_{\mathrm{eq}}(y)$ as given in (38), and is then run to steady state.

Both asymptotic and numerical solutions of the dry model are plotted in Fig. 1, with the following parameter settings:

$$\tau_{\mathrm{eq}} = 20\,\mathrm{days}, \quad \varepsilon = 0.01, \quad \varpi = 0.02, \quad \Lambda = 20\,\mathrm{K}, \quad \sigma = 2.58\,(10\mathrm{N/S}), \quad \overline{T}_{\mathrm{eq}} = 287\,\mathrm{K}. \tag{67}$$

The asymptotic solution has a cell width in close agreement with the numerical solution's width, and the temperature (Fig. 1a) and meridional wind with $\varpi \sim 1$ (Fig. 1b) are nearly indistinguishable from the numerical solutions. The meridional wind with $\varpi \sim \varepsilon$ (Fig. 1b) is close to the numerical solution but slightly weaker. The accuracy of the $\varpi \sim \varepsilon$ dry solution demonstrated here is used to justify scaling ϖ as ε in the moist model. The angular-momentum-conserving asymptotic solution has a discontinuity in the zonal winds at the cell boundary (Fig. 1c), whereas the numerical solution's zonal wind maximizes at slightly smaller $|y|$ and then goes to zero smoothly, but the two are otherwise in very close agreement. The surface zonal winds (Fig. 1d) in both solutions are much weaker than the zonal winds aloft, as assumed in the construction of the asymptotic solutions, and have easterlies near the equator and westerlies further poleward, as in the observations. The near-equatorial surface easterlies in the asymptotic solution are slightly stronger than those in the numerical solution but are broadly in good agreement, and the $\varpi \sim \varepsilon$ surface winds again are weaker but still close to the numerical solution. From this comparison with the numerical solutions, the asymptotic solution is found to successfully capture the dry two-mode solution.

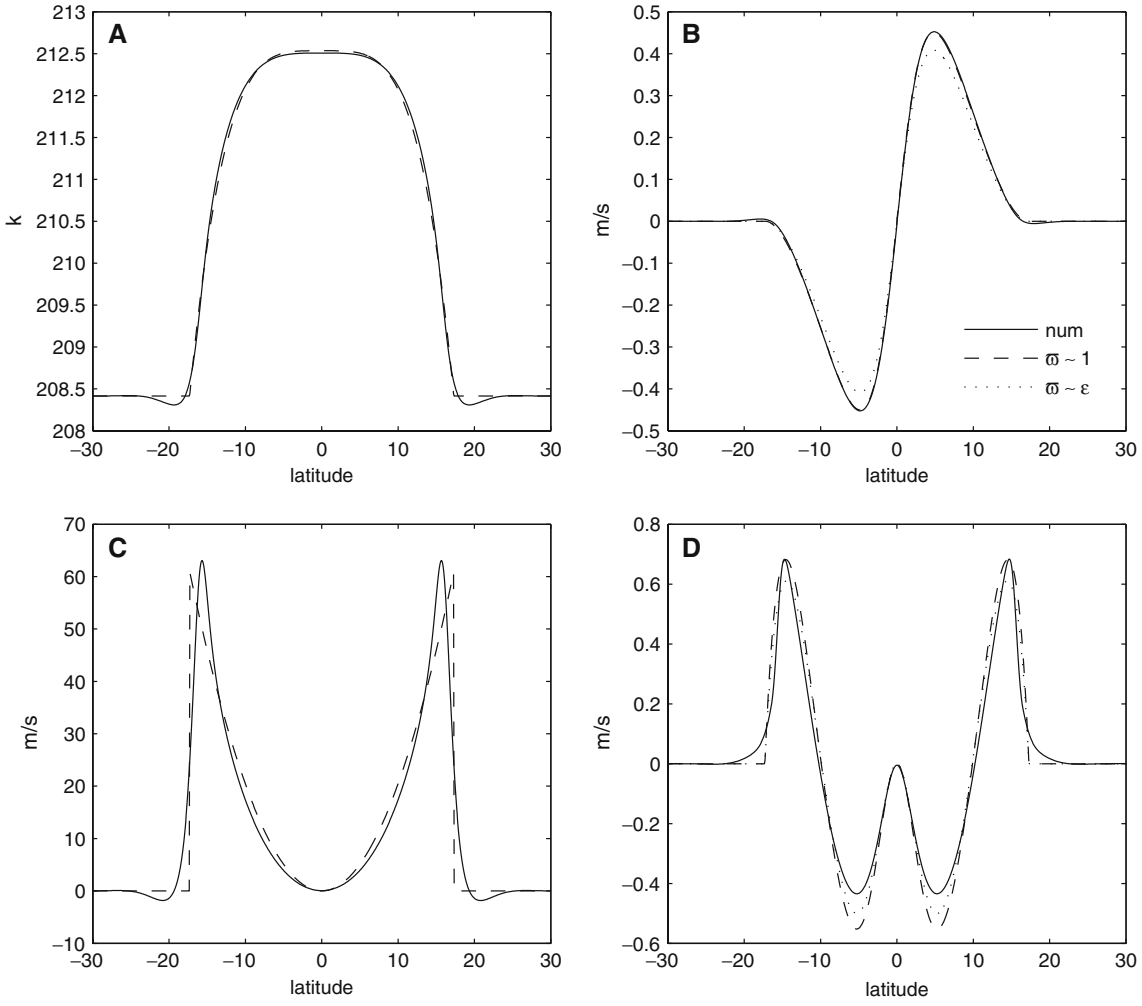

Fig. 1 Dry axisymmetric solutions: *solid* numerical solution, *dashed* asymptotic solution with $\varpi \sim 1$, *dotted* asymptotic solution with $\varpi \sim \varepsilon$. *a* Temperature, *b* meridional wind, *c* zonal wind at the tropopause, *d* surface zonal wind

6 Moist solution with surface drag

Having solved the dry equations, we turn towards a model where moisture is explicitly represented. In addition to equations (6a), (6c), (6d) and (11), the moist model includes the moisture equation (6f), and the full temperature equation (6e) with the explicit representation of convective heating. The asymptotic analysis of the moist model developed below follows the same steps as in the dry model. In particular the solutions for u_1, u_0 and T_1 are identical to those found in the dry model, as moisture only affects the solution of v_1 (and of course q_1).

6.1 Scale analysis and nondimensionalization

The scales for u_1, u_0, v_1 and T_1 are the same as those described in the dry model, and moisture is nondimensionalized by

$$q_1 = \widetilde{Q}\, q_1^*, \tag{68}$$

where $\widetilde{Q}$ is the dimensional scale and q_1^* is the nondimensionalized moisture. The saturation vapor pressure function $q_{\mathrm{sat}}(\mathrm{SST}(y))$ in the evaporation term of (6f) is also be assumed to also scale as $\widetilde{Q}$,

$$q_{\mathrm{sat}} = \widetilde{Q}\, q_{\mathrm{sat}}^*. \tag{69}$$

In the dry problem there is a single timescale $\tau_{\rm eq}$ that represents the total forcing in the system. In the moist model this forcing is divided into radiative cooling, convective heating and surface evaporation with the convective time scale $\tau_{\rm C}^*$ much shorter (12 h) than the surface flux time scale τ_E (7 days) or the radiative time scale $\tau_{\rm R}$ (30 days). Because of the relatively small value of $\tau_{\rm C}^*$, q_1 is close in value to T_1 in convecting regions, and as a result the moisture scale in the convecting regions (where $\mathscr{H}(q_1 - T_1) = 1$) is assumed to be equal to the temperature scale,

$$\widetilde{Q} = \widetilde{T} \qquad \text{(in convecting regions)}. \tag{70}$$

In the nonconvecting regions (where $\mathscr{H}(q_1 - T_1) = 0$) the nondimensional moisture equation (6f) is

$$-\mu_M \frac{\partial}{\partial y^*}\left\{v_1^* + \frac{M_{qp1}}{M_{qr1}}\,\widetilde{Q}\,v_1^*\,q^*\right\} = \frac{\widetilde{Q}}{\widetilde{T}}\frac{\tau_{\rm R}}{\tau_{\rm E}}\left[1 + \frac{\eta^2}{V_s^2}\,U^2(u_s^{*2} + \delta^2 v_s^{*2})\right]^{\frac{1}{2}}\left\{q^*_{\rm sat}({\rm SST}(y^*)) - q_s^*\right\}. \tag{71}$$

In order for the evaporation term on the RHS of (71) be of order one, the moisture scale is set equal to the temperature scale, so that

$$\widetilde{Q} = \widetilde{T} \qquad \text{(in nonconvecting regions)} \tag{72}$$

as well, and it is assumed that $\tau_{\rm R}/\tau_{\rm E} \sim 1$. The scalings (70) and (72) imply that, when the WTG approximation is made, horizontal moisture advection is neglected as well as horizontal temperature advection. This is not valid under all circumstances, as moisture is not subject to the same dynamical constraints as temperature and its horizontal advection can be important even when temperature is not (e.g., [23]).

The nondimensional momentum equations for the moist model, which are unchanged from the dry model as they are not explicitly coupled to q_1, are (46a), (46b) and (46c), the combined zonal momentum equation is (54), and the moist temperature and moisture equations are, respectively:

$$\begin{cases} \dfrac{\partial}{\partial y^*}\left\{v_1^* + \varpi\, v_1^* T_1^*\right\} = \dfrac{\tau_{\rm R}}{\tau_{\rm c}^*}\mathscr{H}(q_1^* - T_1^*)\left[q_1^* - T_1^*\right] + T_{\rm R}^*(y) - T_1^*, & \text{(a)} \\ -\dfrac{\partial}{\partial y^*}\left\{\mu_M v_1^* + \mu_m \varpi\, v_1^* q_1^*\right\} & \text{(b)} \\ \quad = \dfrac{\tau_{\rm R}}{\tau_{\rm c}^*}\mathscr{H}(q_1^* - T_1^*)\left[T_1^* - q_1^*\right] + \dfrac{\tau_{\rm R}}{\tau_{\rm E}}\left[1 + \eta'^2\,(u_s^{*2} + \delta^2 v_s^{*2})\right]^{\frac{1}{2}}\left\{q^*_{\rm sat}({\rm SST}) - b_{1s} q_1^*\right\}, \end{cases} \tag{73}$$

where $\eta' \equiv \eta\,\widetilde{U}/V_s$ is a dimensionless parameter, $\mu_M \equiv M_{\rm qr1}/M_{\rm Sr1}$, $\mu_m \equiv M_{\rm qp1}/M_{\rm Sp1}$, $b_{1s} = b(p_s)$ and the WTG number ϖ is defined in (52). The convective heating term $\left[q_1 - T_1\right]$ in (73a) and the corresponding convective drying term in (73b) are generally smaller than T_1 or q_1, but $\tau_{\rm R}$ is an order of magnitude greater than $\tau_{\rm C}^*$, so that the convective forcing terms are of order one. As for the boundary conditions on T_1^* and q_1^* at $Y_{\rm H}$, they are set to their nondimensional radiative–convective equilibrium values,

$$T_1^*(Y_{\rm H}) = T^*_{\rm RCE} \qquad \text{and} \qquad q_1^*(Y_{\rm H}) = Q^*_{\rm RCE}. \tag{74}$$

The values of $T_{\rm RCE}$ and $Q_{\rm RCE}$ are found by solving (73a) and (73b) for $|y| \geq Y_{\rm H}$ with $v_1^* = \partial v_1^*/\partial y^* = 0$ and $u_1^* = u_0^* = 0$, yielding

$$\begin{aligned} T^*_{\rm RCE} &= \frac{(\tau_{\rm C}^*\, b_{1s} + \tau_{\rm E})\, T_{\rm R}^* + \tau_{\rm R}\, q^*_{\rm sat}(|y^*| \geq Y_{\rm H})}{\tau_{\rm E} + (\tau_{\rm R} + \tau_{\rm C}^*)\, b_{1s}}, \qquad \text{(a)} \\ Q^*_{\rm RCE} &= \frac{(\tau_{\rm C}^* + \tau_{\rm R})\, q^*_{\rm sat}(|y^*| \geq Y_{\rm H}) + \tau_{\rm E} T_{\rm R}^*}{\tau_{\rm E} + (\tau_{\rm R} + \tau_{\rm C}^*)\, b_{1s}}. \qquad \text{(b)} \end{aligned} \tag{75}$$

As in the dry model, it is assumed that $\varepsilon = \tau_D \widetilde{V}/(\widetilde{L}) \ll 1$. Since we have already shown that the dry model, to leading order, is qualitatively unchanged by excluding the WTG terms (cf. Fig. 1), ϖ is chosen to be small in the moist model as well

$$\varpi \sim \varepsilon \ll 1. \tag{76}$$

Also, for simplicity, The radiative equilibrium temperature in equation (73a) is set to a constant value

$$T_{\mathrm{R}}^{*} = R^{*}. \tag{77}$$

For convenience, the function $q_{\mathrm{sat}}^{*}(\mathrm{SST}(y^{*}))$ in equation (73b) is prescribed directly rather than prescribing the SST distribution (because of the nonlinearity of the Clausius–Clapeyron relation, prescribing a simple analytical form for SST does not generally result in a similarly simple form for q_{sat}). Thus we set

$$q_{\mathrm{sat}}^{*}(y^{*}) = \Xi^{*}\,\mathrm{sech}^{2}(\sigma y^{*}) + q_{0}^{*}, \tag{78}$$

where Ξ, σ, and q_0 are constants.

6.2 Asymptotic solutions

As already mentioned, the solutions for u_1, u_0 and T_1 are same as those of the dry model and are given by (61a), (61b) and (61c), except for the value of $T_1^{(0)}(0)$ which is found by applying the radiative–convective equilibrium boundary condition (74) to the temperature solution (61c), resulting in

$$T_1^{(0)}(0) = \frac{\mu}{8}\,Y_{\mathrm{H}}^{4} + T_{\mathrm{RCE}}^{*}. \tag{79}$$

The remaining part of the solution to the moist model consists of finding v_1^{*} and q_1^{*}. Due to the Heaviside functions in equations (73a) and (73b) the moist model must be solved separately in the convecting (with subscript C) and nonconvecting (with subscript NC) regions. The two regions are matched with the condition that v_1 and its first derivative are continuous so that the divergence is finite. The solution for q_1 is continuous by construction. The boundary between the two solutions is determined as the point at which $q_1 = T_1$. In the nonconvecting region, the convective drying term [involving $T_1 - q_1$ in (6e)] vanishes, while in the convecting region it continuously approaches zero as the boundary is approached. Since this term constitutes the only difference in the moisture equation between the two regions, v_1 and q_1 are continuous at the boundary. However, because the model neglects the horizontal advection of moisture to leading order, $\partial q_1/\partial y$ may be discontinuous.

6.2.1 The convecting solutions

In the convecting region the temperature equation (73a) at order $O(\varepsilon^{0})$ is

$$\frac{\partial v_C^{(0)}}{\partial y^{*}} = \frac{\tau_{\mathrm{R}}}{\tau_{\mathrm{C}}^{*}}\left\{q_{\mathrm{C}}^{(0)} - T_1^{(0)}\right\} + R^{*} - T_1^{(0)}, \tag{80}$$

and the moisture equation (73b) at order $O(\varepsilon^{0})$ is

$$-\mu_M\,\frac{\partial v_C^{(0)}}{\partial y^{*}} = \frac{\tau_{\mathrm{R}}}{\tau_{\mathrm{C}}^{*}}\left\{T_1^{(0)} - q_{\mathrm{C}}^{(0)}\right\} + \frac{\tau_{\mathrm{R}}}{\tau_{\mathrm{E}}}\left(q_{\mathrm{sat}}^{*} - b_{1s}q_{\mathrm{C}}^{(0)}\right), \tag{81}$$

where the leading order zero zonal surface wind result (56) has been used in the evaporation term. Eliminating $\partial v_C^{(0)}/\partial y^{*}$ between (80) and (81), the solution for the moisture in the convecting region is

$$q_C^{(0)} = \gamma_1\left\{\mu_M\frac{\tau_{\mathrm{C}}^{*}}{\tau_{\mathrm{R}}}\,R^{*} + \frac{\tau_{\mathrm{C}}^{*}}{\tau_{\mathrm{E}}}\,q_{\mathrm{sat}}^{*} + \gamma_2 T_1^{(0)}\right\}, \tag{82}$$

with $\gamma_1 \equiv 1 - \mu_M + b_{1s}\tau_{\mathrm{C}}^{*}/\tau_{\mathrm{E}}$, and $\gamma_2 \equiv 1 - \mu_M - \mu_M\tau_{\mathrm{C}}^{*}/\tau_{\mathrm{R}}$. The solution for the meridional velocity in the convecting region, using boundary condition (15b), is then

$$v_C^{(0)} = \gamma_1\left\{\gamma_3\,R^{*}\,y^{*} + \frac{\tau_{\mathrm{R}}}{\tau_{\mathrm{E}}}\left[\frac{\Xi^{*}}{\sigma}\tanh(\sigma y^{*}) + q_0^{*}\,y^{*}\right] + \left(\gamma_3 + b_{1s}\frac{\tau_{\mathrm{R}}}{\tau_{\mathrm{E}}}\right)\left[\frac{\mu}{40}\,y^{*5} - T_1^{(0)}(0)\,y^{*}\right]\right\}, \tag{83}$$

with $\gamma_3 \equiv 1 + b_{1s}\tau_{\mathrm{C}}^{*}/\tau_{\mathrm{E}}$. Recall that the $T_1^{(0)}$ terms in (82) and (83) involve the unknown width Y_{H} of the Hadley cell, via (79) and (61c).

6.2.2 The nonconvecting solution

In the nonconvecting region the temperature equation (73a) at order $O(\varepsilon^0)$ is

$$\frac{\partial v_{\rm NC}^{(0)}}{\partial y^*} = R^* - T_1^{(0)}, \tag{84}$$

and the moisture equation (73b) at order $O(\varepsilon^0)$ is

$$-\mu_M \frac{\partial v_{\rm NC}^{(0)}}{\partial y^*} = \frac{\tau_{\rm R}}{\tau_{\rm E}} \left(q_{\rm sat}^*({\rm SST}) - b_{1s} q_{\rm NC}^{(0)}\right), \tag{85}$$

where the leading order zero zonal surface wind result (56) has again been used in the evaporation term. Solving (84) yields

$$v_{\rm NC}^{(0)} = \int_0^{y^*} \left(R^* - T_1^{(0)}\right) {\rm d}\acute{y} = R^*\, y^* + \frac{\mu}{40}\, y^{*5} - T_1^{(0)}(0)\, y^* + c_{\rm NC}, \tag{86}$$

where $c_{\rm NC}$ is determined by the condition $v_C^{(0)}(Y_{\rm P}) = v_{\rm NC}^{(0)}(Y_{\rm P})$. Finally, the solution for q_1 in the nonconvecting region is found using (84) and (85) resulting in

$$q_{\rm NC}^{(0)} = \frac{\mu_M}{b_{1s}} \frac{\tau_{\rm E}}{\tau_{\rm R}} \left(R^* - T_1^{(0)}\right) + \frac{q_{\rm sat}^*}{b_{1s}}. \tag{87}$$

6.3 The widths of the convecting region and the Hadley cell

The width of the ITCZ, $Y_{\rm P}$, is found first by locating the point at which $q_1 = T_1$. The solution for $Y_{\rm P}$ is determined by equating the temperature solution (61c) and the moisture solution (87),

$$\mu_M \frac{\tau_{\rm E}}{\tau_{\rm R}} R^* - \gamma_4 \Big[-\frac{\mu}{8}\, y^{*4} + T_1^{(0)}(0) \Big] + \Xi^* \,{\rm sech}^2(\sigma y^*) + q_0^* = 0, \tag{88}$$

where $\gamma_4 \equiv b_{1s} + \mu_M \tau_{\rm E}/\tau_{\rm R}$ and $T_1^{(0)}(0)$, as defined in (79), is a function of $Y_{\rm H}$. Solving (88) numerically gives four roots that are all real and come in positive and negative pairs. The first pair are real and give the value of $Y_{\rm P}$ on either side of the equator. The second pair are also real and within the interval $[0, Y_{\rm H}]$. This second solution, denoted $Y_{\rm B}$, reveals that, in addition to the equatorial convecting region, there is a another small convecting region at the edge of the cell near $Y_{\rm H}$, so that

$$0 < Y_{\rm P} < Y_{\rm B} < Y_{\rm H}. \tag{89}$$

These regions are illustrated in Fig. 2. Solutions labeled 'C' correspond to the convecting ITCZ which begins at the equator and ends at $Y_{\rm P}$. Solutions in the nonconvecting region of the Hadley circulation, labeled 'NC', start at $Y_{\rm P}$ and extend to $Y_{\rm B}$, which is close to $Y_{\rm H}$. Solutions in the narrow precipitating boundary region are labeled B. A radiative–convective equilibrium region lies outside of $Y_{\rm H}$ where there is no flow. The expression for $v_{\rm B}^{(0)}$ is identical to $v_{\rm C}^{(0)}$ in (83) except for the constant c_B determined by matching $v_{\rm B}^{(0)}(Y_{\rm B}) = v_{\rm NC}^{(0)}(Y_{\rm B})$, and the expression for $q_B^{(0)}$ is identical to the one for $q_C^{(0)}$ in (82),

$$\begin{aligned} q_B^{(0)} &= q_C^{(0)}, \qquad (a) \\ v_B^{(0)} &= v_C^{(0)} + c_B. \qquad (b) \end{aligned} \tag{90}$$

An approximate expression for $Y_{\rm P}$ can be found from (88) assuming that $Y_{\rm p}$ is within one deformation radius of the equator, or in nondimensional terms, $Y_{\rm P} < 1$. With this assumption, the $Y_{\rm P}^4$ term in (88) is neglected and a solution for $Y_{\rm P}$ can be written, approximately,

$$Y_{\rm P} \approx \frac{1}{\sigma} \,{\rm sech}^{-1} \left[\sqrt{\frac{1}{\Xi^*} \left\{ \gamma_4 \frac{\mu}{8}\, Y_{\rm H}^4 - \varphi \right\}} \,\right], \tag{91}$$

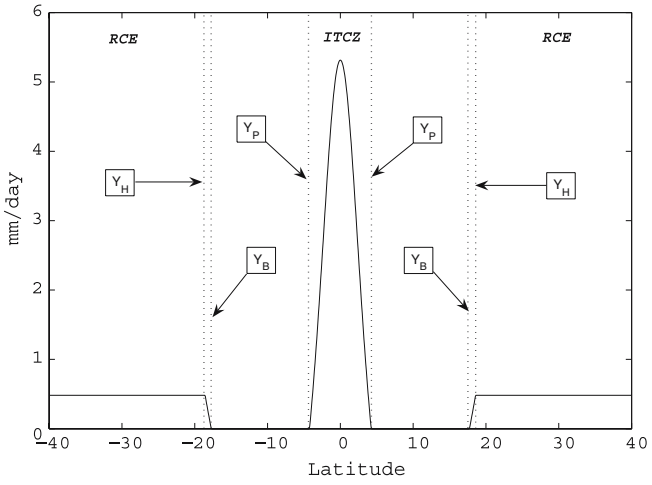

Fig. 2 A schematic of precipitation in the convecting and nonconvecting regions

$$\text{where } \varphi \equiv q_0^* + \mu_M \frac{\tau_E}{\tau_R} R^* - \gamma_4 T^*_{RCE}. \tag{92}$$

The inverse hyperbolic secant dependence of Y_P on Y_H here is specific to the forcing used in this model; if a Gaussian-shaped forcing had been used, Y_P would have a logarithmic dependence on Y_H. The second solution to (88) is found by assuming that $\sigma Y_B > 1$ and $\text{sech}^2(\sigma Y_P) \approx 0$. With these assumption, the second solution to (88) is

$$Y_B \approx \left\{ Y_H^4 - \frac{\varphi}{\gamma_4 \frac{\mu}{8}} \right\}^{1/4}. \tag{93}$$

With approximate expressions for $Y_P(Y_H)$ and $Y_B(Y_H)$, a single equation for Y_H can now be constructed from the boundary condition $v_B^{(0)}(Y_H) = 0$, and the conditions that $q_{NC}(Y_P) = T_1(Y_P)$ and $q_B(Y_B) = T_1(Y_B)$, resulting in

$$\Xi^* - \gamma_5 \frac{\mu\,\sigma}{10} Y_H^5 + \left\{ \frac{4}{5}\sigma Y_H \left[1 - \frac{8\varphi}{\mu\gamma_4 Y_H^4} \right]^{1/4} - \frac{1}{2} - \text{sech}^{-1}\left[\sqrt{\frac{1}{\Xi^*}\left(\gamma_4 \frac{\mu}{8} Y_H^4 - \varphi \right)} \right] \right\} \left(\gamma_4 \frac{\mu}{8} Y_H^4 - \varphi \right) = 0, \tag{94}$$

where $\gamma_5 \equiv \tau_E/\tau_R + b_{1s}(\tau_C^*/\tau_R + 1)$. In order to derive an expression for Y_H from (94), the inverse hyperbolic secant term, which comes from the expression for Y_P, is expanded in a power series about $(1/\Xi^*)(\gamma_4\mu Y_H^4/8 - \varphi) = 1$, which corresponds to expanding about the equator ($y^* = 0$). Retaining only the leading term yields

$$\text{sech}^{-1}\left[\sqrt{\frac{1}{\Xi^*}\left(\gamma_4 \frac{\mu}{8} Y_H^4 - \varphi \right)} \right] \approx 2\sqrt{1 - \left[\frac{2\gamma_4\mu}{\varphi + \Xi^*} \right]^{1/4} \frac{Y_H}{2}}, \tag{95}$$

which is further approximated using a binomial expansion for the RHS, resulting in

$$2\sqrt{1 - \left[\frac{2\gamma_4\mu}{\varphi + \Xi^*} \right]^{1/4} \frac{Y_H}{2}} \approx 2 - \left[\frac{2\gamma_4\mu}{\varphi + \Xi^*} \right]^{1/4} \frac{Y_H}{2}. \tag{96}$$

The term $(1 - 8\varphi/(\mu\gamma_4 Y_H^4))^{1/4}$ in (94) is then approximated by assuming $\gamma_4\mu Y_H^4/8 > \varphi$, and using a binomial expansion, so that

$$\left[1 - \frac{8\varphi}{\mu\gamma_4 Y_H^4} \right]^{1/4} \approx 1 - \frac{2\,\varphi}{\gamma_4\,\mu Y_H^4}. \tag{97}$$

Substituting (95), (96) and (97) in (94), yields a polynomial in $Y_{\rm H}$ of degree eight, which can be further approximated into the quartic

$$\frac{5}{16}\,\gamma_4\mu\,Y_{\rm H}^4+\left\{\sigma+\frac{1}{2}\left[\frac{2\gamma_4\mu}{\varphi+\Xi^*}\right]^{1/4}\right\}\varphi\,Y_{\rm H}-\left(\Xi^*+\frac{5}{2}\,\varphi\right)=0, \tag{98}$$

by neglecting terms with small coefficients. Finally, this quartic has only one real positive solution, with the approximate form

$$Y_{\rm H}\approx 2\left\{\frac{\Xi^*+\frac{5}{2}\,\varphi}{5\,\gamma_4\mu}\right\}^{1/4}-\frac{4}{5}\,\frac{\varphi\,\sigma}{\sqrt{5\,\gamma_4\mu\left(\Xi^*+\frac{5}{2}\,\varphi\right)}}. \tag{99}$$

Having obtained approximate analytic solutions, we now examine the sensitivity to the different parameters of the model. The values of $Y_{\rm H}$, $Y_{\rm P}$ and $Y_{\rm B}$ are numerically calculated by solving (88) and the boundary condition $v_B^{(0)}(Y_{\rm H})=0$, and these solutions are plotted in Fig. 3 and 4. The approximate analytic solutions using (99) for $Y_{\rm H}$, (91) for $Y_{\rm P}$ and (93) for $Y_{\rm B}$ are plotted in Fig. 5. The values of the parameters varied in Fig. 3, 4, 5 are normalized by the following values

$$\begin{aligned}&\tau_{\rm C}=0.5\,{\rm d},\quad \tau_{\rm R}=30\,{\rm d},\ \tau_{\rm E}=7.7\,{\rm d},\quad R=272\,{\rm K},\\ &\Xi=8\,{\rm K},\quad \sigma=2.58\,(10{\rm N/S}),\quad q_0=-6.03\ {\rm K}\,({\rm SST}=295\,{\rm K}),\end{aligned} \tag{100}$$

which are used in the full nonlinear numerical solution of the model, described in the Sect. 6.4 below.

In Fig. 3a, $Y_{\rm P}$ is plotted versus $\tau_{\rm C}^*,\ \tau_{\rm R},\ \tau_{\rm E}$ and R. $Y_{\rm P}$ is significantly sensitive to $\tau_{\rm C}^*$, and has a finite width for $\tau_{\rm C}^*=0$ (not shown here). As $\tau_{\rm C}^*$, decreases the value of the moisture is relaxed more strongly to the temperature, whose solution is independent of the moisture (61c) and in the limit that $\tau_C^*\to 0$, the moisture and temperature are equal. $Y_{\rm P}$ is also sensitive to R, is inversely proportional to $\tau_{\rm R}$ and is relatively insensitive to $\tau_{\rm E}$ with a change of only a few tenths of a degree over all values of $\tau_{\rm E}$. In Fig. 3b the sensitivity of $Y_{\rm H}$ to $\tau_{\rm C}^*,\ \tau_{\rm R},\ \tau_{\rm E}$ and R is plotted. $Y_{\rm H}$ is inversely proportional to $\tau_{\rm C}^*,\ \tau_{\rm E}$ and R and is directly proportional to $\tau_{\rm R}$.

The numerically computed sensitivities of $Y_{\rm P}$, $Y_{\rm H}$ and $Y_{\rm B}$ to the parameters of the SST forcing are plotted in Fig. 4. In Fig. 4a the the sensitivity of $Y_{\rm P}$ and $Y_{\rm B}$ to Ξ and σ are plotted. $Y_{\rm P}$ is relatively insensitive to increasing Ξ,σ, but increases slightly for small values of Ξ and σ. Both $Y_{\rm P}$ and $Y_{\rm B}$ are insensitive to varying q_0, which is not plotted here. For values of $\Xi<3.6$, $Y_{\rm B}$ and $Y_{\rm P}$ meet, the nonconvecting region disappears and the atmosphere is convecting throughout the domain. A similar transition between solutions with convection everywhere and ones with a nonconvective region as the SST contrast was increased was found for nonrotating Walker-circulation solutions by Bretherton and Sobel [1]. Here, the solution with convection everywhere persists to a larger SST contrast than in that study. While the two systems cannot be precisely compared, due to

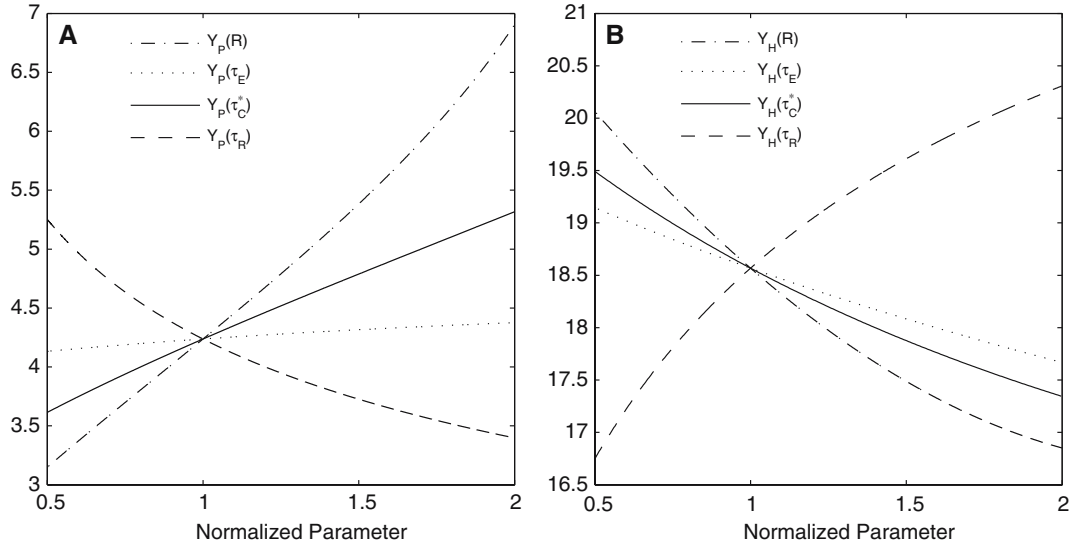

Fig. 3 The sensitivity of $Y_{\rm P}$ and $Y_{\rm H}$, expressed in latitude, to time scales and R computed numerically

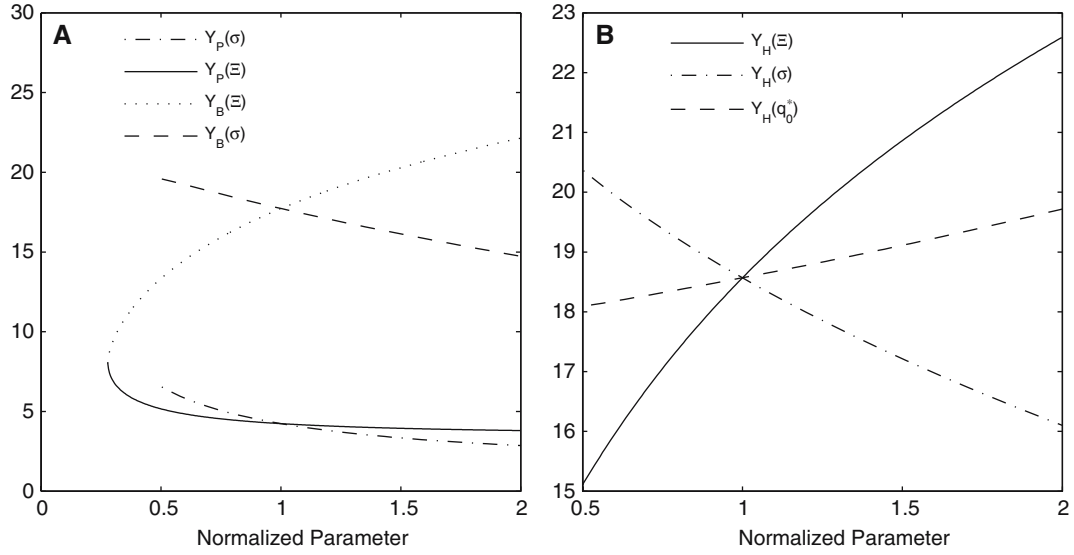

Fig. 4 The sensitivity of Y_P, Y_B and Y_H, expressed in latitude, to SST forcing parameters computed numerically

the different boundary conditions and forms for the SST profiles, we nonetheless speculate that this difference is due primarily to the presence of a nonzero Coriolis parameter in the present case and the lack of the same in Bretherton and Sobel [1]. The sensitivity of Y_H is plotted in the Fig. 4b: the cell size decreases as the height of the SST forcing decreases (decreasing Ξ), and as the width of forcing decreases (increasing σ). Y_H is relatively insensitive to q_0, the constant term in (78), which sets the value of the SST outside of the cell.

The sensitivities of the approximate analytic solutions for Y_H, Y_P and Y_B to the SST forcing parameters is plotted in Fig. 5. In Fig. 5a, Y_P and Y_B are plotted as functions of Ξ and σ . The sensitivities to q_0 again are not plotted, as Y_P and Y_B are only weak functions of q_0. In Fig. 5b, Y_H as a function of Ξ, σ and q_0 is plotted. These plots show that the approximate analytical expressions are able to capture the correct size of the of Y_P, Y_H and Y_B and the direction of change for the varied parameters, but slightly weaker sensitivities than the numerical solutions. These sensitivities have also been computed without the second term on the RHS of (99), but this term is essential to capturing the correct parameter dependence of Y_H.

Some of the parameter dependencies are easily understood. Y_H increases as a function of the forcing strength, Ξ, and decreases, albeit weakly, as a function of forcing width, σ; increasing σ decreases the magni-

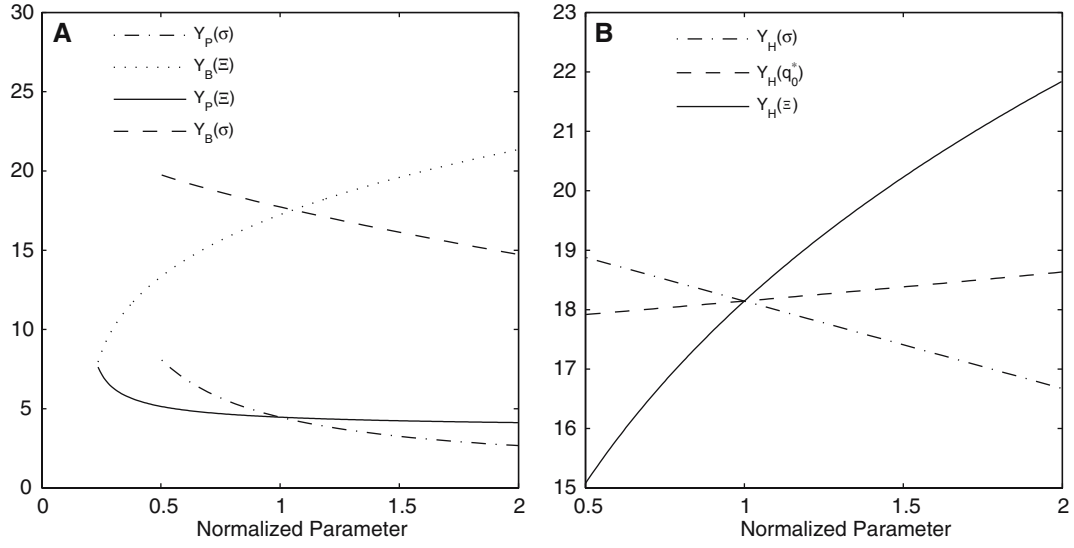

Fig. 5 The sensitivity of Y_P, Y_B and Y_H, expressed in latitude, to SST forcing parameters from the approximate analytic expressions

tude of the SST gradients, which ultimately (if indirectly) are the forcing for the meridional pressure gradients. The sensitivities of Y_P to the SST profile parameters are not so transparent, but are in any case small. Of the diabatic forcing parameters shown in Fig. 3, Y_P is most sensitive to R, and secondly to τ_c and τ_R. We do not have simple physical arguments for these sensitivities. The sensitivities of Y_B are qualitatively similar to those of Y_H; we do not attempt to analyze the changes in the width of the boundary region, $Y_H - Y_B$.

6.4 Comparison with numerical solution

A numerical solution for the moist model is found using the same numerical code described in the dry model (Sect. 5.4) but with equation (12) replaced by (73a) and (73b). The asymptotic and numerical solutions are plotted in Fig. 6 with the parameter values defined in (100) of Sect. 6.3. For these parameter values, $\varepsilon = 7 \times 10^{-3}$

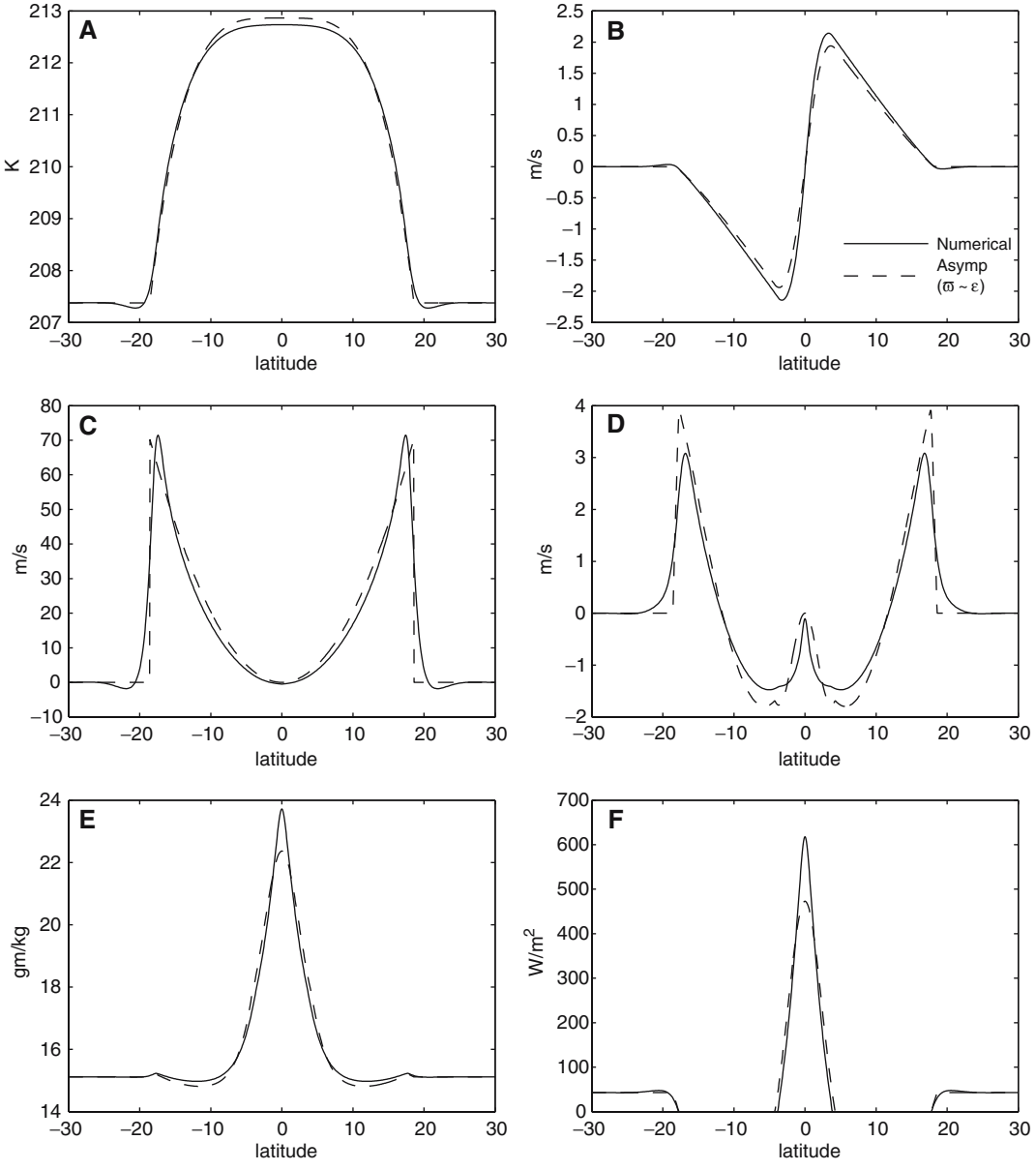

Fig. 6 Moist axisymmetric solutions: *solid* numerical solution, *dashed* asymptotic solution with $\varpi \sim \varepsilon$. *a* Temperature at the tropopause, *b* meridional wind at the tropopause, *c* zonal wind at the tropopause, *d* surface zonal wind, *e* surface moisture and *f* precipitation

and $\varpi = 2 \times 10^{-2}$, which are consistent with the small parameter assumptions. The width of the moist asymptotic solution's circulation nearly equals the numerical solution's width. The asymptotic solution's temperature (Fig. 6a) is slightly greater near the equator but captures the width of the full numerical solution, and the asymptotic meridional winds at the tropopause (Fig. 6b) are also very close to the numerical solution but weaker at the maximum and minimum. The asymptotic solution's zonal winds at the tropopause (Fig. 6c) have similar agreement to the numerical solution as in the dry model, and the asymptotic surface zonal winds (Fig. 6d) are slightly stronger than the numerical solution. The asymptotic solution's moisture (Fig. 6e) and precipitation (Fig. 6f) are in agreement with the numerical value of the width of the ITCZ, Y_{P}, but with peak values that are noticeably weaker than those in the numerical results. We believe this discrepancy arises due to the neglect of the moisture dependence of the M_q in the asymptotic solution (the term involving M_{qp1} was found to be $O(\varepsilon)$).

The moist Hadley circulation study of Fang and Tung [5] is similar to ours in its use of the WTG approximation to arrive at an asymptotic solution. Their model differs from the model presented here in their use of a continuously stratified atmosphere and their convective region (ITCZ) is confined to a delta function. The use of a continuous atmosphere allows them to solve for the sloping edge of the Hadley circulation, which is not possible in this two-mode model, but they were unable to obtain a closed expression for the width of the convective region as we have done here. Their strict enforcement of no temperature gradients at leading order lead them to a temperature field that is constant throughout the Hadley circulation and is set by the temperature in the ITCZ. They conclude that the temperature in a moist model of the Hadley circulation is greater than that found in a dry model and that is should lead to a stronger circulation. In the model described here, unlike the Fang and Tung model, the temperature solution allows for small temperature gradients at leading order. The meridional circulation is slightly stronger in the moist model compared to the dry model, but the temperature solutions for the dry and moist models are nearly identical though it is not immediately obvious how to compare the forcings between the two models.

7 Conclusions

The model discussed in this study occupies the space in the hierarchy of axisymmetric atmospheric models between numerical models with continuous stratification and simpler one-mode shallow water models, and is capable of predicting the winds, temperature, moisture and width of the cell and ITCZ of the circulation. Our analysis of the QTCM equations shows that the barotropic and baroclinic modes cancel at the surface due to the strong surface drag and interact constructively near the tropopause. This arrangement of the momentum modes enables the model to have both weak surface winds and strong, angular momentum conserving winds aloft, as in fully stratified axisymmetric models of the Hadley circulation. In the asymptotic analysis discussed above, angular-momentum conservation occurs at an order in ε which differs from that of the nonzero correction to the surface winds (which is found at next order). This separation of the surface winds and angular momentum conservation is only possible by making the assumption that $\lambda \sim \varepsilon^{1/2}$ in the combined momentum equation (54), a slightly nonstandard step since λ depends on the vertical structure functions of the model and cannot strictly be viewed as variable, i.e., it cannot literally be sent to zero as strictly required by the principles of asymptotic analysis.

The results here show that the weak temperature gradient approximation (at least in the same loosened form used by [16]) is valid for studying the Hadley circulation and enables the moist model to be solved using asymptotic methods. The results of the dry model show that the inclusion of horizontal advection of temperature is not essential to capture the dynamics of the two-mode Hadley cell. In the moist model, horizontal moisture advection can also be neglected without great damage to the solutions. This is in contrast to the results of Bretherton and Sobel [1] for the nonrotating Walker circulation. In that context, horizontal moisture advection was found to play an important role in setting the location of the boundary between convective and nonconvective regions.

This two-mode model is capable of generating an ITCZ whose width and strength are broadly comparable to those observed in the absence of horizontal diffusion. This is in contrast to the model presented by Sobel and Neelin (this volume), whose free troposphere is essentially the same as our model here but which adds a near-surface boundary layer. In that model, configured axisymmetrically as here, horizontal diffusion is needed to prevent the ITCZ from becoming very intense and narrow.

Acknowledgments This work was supported by the US National Science Foundation under grant DMS-0139830 and via a Fellowship to Samuel Burns from the IGERT Joint Program in Applied Mathematics and Earth and Environmental Science at Columbia University. We are grateful to the members of the Focused Research Group on tropical dynamics, J. A. Biello and M. A. Wittman for useful discussions.

Appendix

Table 1 Definition of variables, parameters and constants

Symbol	Description	Value	Units
y	Latitude	Variable	[m]
$u_0,\ u_1$	Zonal barotropic and baroclinic winds	Variables	[m/s]
$v_0,\ v_1$	Meridional barotropic and baroclinic winds	Variables	[m/s]
$T_1,\ q_1$	Baroclinic temperature and moisture	Variables	[J/kg]
$T_{\rm eq}$	Equilibrium temperature profile	Parameter	[J/kg]
$T_{\rm RCE},\ Q_{\rm RCE}$	Radiative–convective equilibrium temperature and moisture	Variable	[J/kg]
$T_{\rm R}$	Radiative equilibrium temperature profile	Parameter	[J/kg]
$Y_{\rm H},\ Y_{\rm C},\ Y_{\rm B}$	Width of the Hadley circulation, convecting region and boundary region	Variables	[m]
α_1	$\langle V_1^3\rangle/\langle V_1^2\rangle$	0.25	[1]
α_2	$\langle V_1\Omega_1\partial_p V_1\rangle/\langle V_1^2\rangle$	7.1×10^{-2}	[1]
α_3	$(\alpha_1-\alpha_2)/2$	9.0×10^{-2}	[1]
α_4	$\alpha_1+\alpha_2$	0.32	[1]
λ	$-(\alpha_2+V_{1s})$	0.17	[1]
Ω	Rate of rotation of the Earth	7.29×10^{-5}	[1/s]
$r_{\rm Earth}$	Radius of the Earth	6.38×10^{6}	[m]
f	Coriolis parameter ($2\Omega\sin(y/r_{\rm Earth})$)	Parameter	[1/s]
β	Variation of f with latitude ($2\Omega/r_{\rm Earth}$)	2.29×10^{-11}	[1/(s m)]
ε	$\tau_D\widetilde{V}/\widetilde{L}$	Parameter	[1]
δ	$\widetilde{V}/\widetilde{U}$	Parameter	[1]
V_{1s}	Surface value of the baroclinic vertical velocity profile	-0.24	[1]
c	QTCM gravity-wave speed ($\sqrt{\kappa M_{Sr1}/\widehat{a}_1}$)	47.7	[m/s]
κ	R^*/c_p	2.86×10^{-1}	[1]
$\tau_{\rm eq}$	Equilibrium temperature time scale	Parameter	[1/s]
$\tau_{\rm C},\ \tau_{\rm R},\ \tau_{\rm E},\ \tau_{\rm D}$	Time scales for convection, radiation, evaporation and surface drag	Parameter	[1/s]
τ_C^*	$\frac{1}{\tau_c}\widehat{a}_1\widehat{b}_1/(\widehat{a}_1+\widehat{b}_1)$	Parameter	[1/s]
M_{Sr1}	Reference value of the dry static stability	3.5×10^{3}	[J/kg]
M_{Sp1}	Change in the dry static stability per T_1 change	3.4×10^{-2}	[1]
M_{qr1}	Reference value of the gross moisture stratification	3.0×10^{3}	[J/kg]
M_{qp1}	Change in the gross moisture stratification per q_1 change	2.7×10^{-2}	[1]
η	Weighting of the actual surface-wind contribution to the evaporation	Parameter	[1]
η'	$\eta\widetilde{U}/V_s$	Parameter	[1]
V_s	Average surface-wind speed	10.0	[m/s]
$q_{\rm sat}$	Surface moisture saturation vapor pressure	Parameter	[J/kg]
$u_s,\ v_s,\ T_s,\ q_s$	Surface values of zonal and meridional wind, temperature and moisture	Variables	[m/s], [J/kg]
ϖ	Weak temperature gradient number, $(M_{Sp1}/M_{Sr1})\,\tilde{T}$	Parameter	[1]
Ro	Rossby number	1.0	[1]
Ek	Ekman number	Parameter	[1]
μ	$1/(\alpha_4-V_{1s})$	1.8	[1]
μ_M	M_{qr1}/M_{Sr1}	0.86	[1]
μ_m	M_{qp1}/M_{Sp1}	0.79	[1]
b_{1s}	$b(p_s)$	1.0	[1]
R	Constant value used for T_R	Parameter	[J/kg]
$a_1(p),\ b_1(p)$	Vertical profiles of temperature and moisture	Constant	[1]
Ξ	Amplitude of SST saturation vapor pressure	Parameter	[J/kg]
q_0	Constant term in the SST vapor pressure	Parameter	[J/kg]
C_D	Bulk coefficient	1.0×10^{-3}	[1]
ρ_a	Density of air at sea level	1.23	[kg/m^3]
$p_{\rm s}$, $p_{\rm t}$	Pressure at the surface and top of the model	$1.0\times10^{5},\ 2.0\times10^{4}$	[Pa]
p_T	$p_{\rm s}-p_{\rm t}$	8.0×10^{4}	[Pa]
$\widehat{a}_1,\ \widehat{b}_1$	The vertical averages of $a_1(p)$ and $b_1(p)$	0.44, 0.45	[1]
Λ	Amplitude of T_{eq}	Parameter	[J/kg]
σ	Width of $T_{\rm eq}$	Parameter	[1]
$\overline{T}_{\rm eq}$	Value of $T_{\rm eq}$ away from the equator	Parameter	[J/kg]
$v_C,\ q_C$	Convecting solution for meridional velocity and moisture	Variables	[m/s], [J/kg]

Table 1 (contd.)

Symbol	Description	Value	Units
v_{NC}, q_{NC}	Nonconvecting solution for meridional velocity and moisture	Variables	[m/s], [J/kg]
v_{B}, q_{B}	Boundary region solution for meridional velocity and moisture	Variables	[m/s], [J/kg]
γ_1	$1-\mu_M+b_{1s}\tau_C^*/\tau_E$	Parameter	[1]
γ_2	$1-\mu_M-\mu_M\tau_C^*/\tau_R$	Parameter	[1]
γ_3	$1+b_{1s}\tau_C^*/\tau_E$	Parameter	[1]
γ_4	$b_{1s}+\mu_M\tau_E/\tau_R$	Parameter	[1]
γ_5	$\tau_E/\tau_R+b_{1s}(\tau_C^*/\tau_R+1)$	Parameter	[1]
c_{NC}, c_{B}	Momentum integration constants in the nonconvecting and boundary regions	Parameters	[m/s]
φ	$q_0^*+\mu_M\frac{\tau_E}{\tau_R}R-\gamma_4 T_{RCE}$	Parameter	[1]
$\underset{\sim}{(\ )}^*$	Denotes a nondimensionalized variable		
$(\ )$	Denotes a dimensional scale		
$(\ )^{(0,1/2,1,\ldots)}$	Denotes the order in the asymptotic expansion		

References

1. Bretherton, C.S., Sobel, A.H.: A simple model of a convectively-coupled Walker circulation using the weak temperature gradient approximation. J. Climate **15**, 2907–2920 (2002)
2. Burns, S.P., Sobel, A.H.: Radiative feedbacks in idealized, axisymmetric simulations of the moist hadley circulation. J. Atmos. Sci. (submitted) (2006)
3. Fang, I.M., Tung, K.K.: Time-dependent nonlinear hadley circulation. J. Atmos. Sci. **56** (12): 1797–1807 (1999)
4. Fang, I.M., Tung, K.K.: The dependence of the Hadley circulation on the thermal relaxation time. J. Atmos. Sci. **53** (9): 1241–1261 (1997)
5. Fang, I.M., Tung, K.K.: A simple model of nonlinear hadley circulation with an ITCZ: analytic and numerical solutions. J. Atmos. Sci. **54** (10): 1379–1384; **53** (9): 1241–1261 (1996)
6. Gill, A.E.: Some simple solutions for heat-induced tropical circulaton. Q. J. R. Meteor. Soc. **106**, 447–462 (1980)
7. Held, I.M., Hou, A.Y.: Nonlinear axially symmetric circulations in a nearly inviscid atmosphere. J. Atmos. Sci. **37**, 515–533 (1980)
8. Held, I.M., Phillips, P.J.: A barotropic model of the interaction between the Hadley Cell and a Rossby wave. J. Atmos. Sci. **47**, 856–869 (1990)
9. Hsu, C.J., Plumb, R.A.: Nonaxisymmetric thermally driven circulations and upper-tropospheric monsoon dynamics. J. Atmos. Sci. **57**(9): 1255–1276 (2000)
10. Kirtman, B.P., Schneider, E.K.: A spontaneously generated atmospheric general circulation. J. Atmos. Sci. **57** (13): 2080–2093 (2000)
11. Lindzen, R.S., Hou, A.Y.: Hadley circulations for zonally averaged heating centered off the equator. J. Atmos. Sci. **45**, 2416–2427 (1988)
12. Matsuno, T.: Quasi-geostrophic motions in the equatorial area. J. Meteor. Soc. Jpn. **44**, 25–43 (1966)
13. Neelin, J.D., Zeng, N.: A quasi-equilibrium tropical circulation model-formulation. J. Atmos. Sci. **57**, 1741–1766 (2000)
14. Numaguti, A.: Dynamics and energy balance of the hadley circulation and the tropical precipitation zones. part II: sensitivity to meridional SST distribution. J. Atmos. Sci. **52** (8): 1128–1141 (1995)
15. Numaguti, A.: Dynamics and energy balance of the hadley circulation and the tropical precipitation zones: significance of the distribution of evaporation. J. Atmos. Sci. **50** (13): 1874–1887 (1993)
16. Polvani, L.M., Sobel, A.: The Hadley circulation and the weak temperature gradient approximation. J. Atmos. Sci. **59**, 1744–1752 (2002)
17. Satoh, M.: Hadley circulations in radiative-ûconvective equilibrium in an axially symmetric atmosphere. J. Atmos. Sci. **51** (13): 1947–1968 (1994)
18. Schneider, E.K., Lindzen, R.S.: Axially symmetric steady-state models of the basic state for instability and climate studies. Part 1. linearized calculations. J. Atmos. Sci. **34** (2): 263–279 (1977)
19. Schneider, E.K.: Axially symmetric steady-state models of the basic state for instability and climate studies. Part 2. nonlinear calculations. J. Atmos. Sci. **34** (2): 280–296 (1977)
20. Schneider, E.K.: Martian great dust storms: interpretative axially symmetric models. ICARUS **55**, 302–331 (1983)
21. Schneider, E.K.: A simplified model of the modified Hadley circulation. J. Atmos. Sci. **44**, 3311–3328 (1987)
22. Sobel, A.H., Bretherton, C.S.: Large-scale waves interacting with deep convection in idealized mesoscale model simulations. Tellus **55A**, 45–60 (2003)
23. Sobel, A.H.: Water vapor as an active scalar in tropical atmospheric dynamics. Chaos **12**, 451–459 (2002)
24. Sobel, A.H., Nilsson, J., Polvani, L.: The weak temperature gradient approximation and balanced tropical moisture waves. J. Atmos. Sci. **58**, 3650–3665 (2001)
25. Walker, C.C., Schneider, T.: Response of idealized Hadley circulations to seasonally varying heating. Geophys. Res. Lett., **32**, L06813 (2005)
26. Yu, J.Y., Neelin, J.D.: Analytic approximations for moist convectively adjusted regions. J. Atmos. Sci. **54**, 1054–1063 (1997)